Timing of Breakup and Thermal Evolution of a Pre-Caledonian Neoproterozoic Exhumed Magma-Rich Rifted Margin

Hans Jørgen Kjøll, Torgeir B. Andersen, Fernando Corfu, Loic Labrousse, Christian Tegner, Mohamed Mansour Abdelmalak, Sverre Planke

AGU100 ADVANCING EARTH AND SPACE SCIENCE

Tectonics

RESEARCH ARTICLE
10.1029/2018TC005375

Key Points:
- Detailed field observations reveal crustal structures of a well-preserved exhumed magma-rich rifted margin in the Scandinavian Caledonides
- The dike swarm was emplaced at 9- to 16-km depth and introduced significant amounts of heat into the crust causing local crustal anatexis
- U-Pb dating shows that these processes occurred between about 615 and 590 Ma

Supporting Information:
- Supporting Information S1
- Table S1
- Data Set S1

Correspondence to:
H. J. Kjøll,
h.j.kjoll@geo.uio.no

Citation:
Kjøll, H. J., Andersen, T. B., Corfu, F., Labrousse, L., Tegner, C., Abdelmalak, M. M., & Planke, S. (2019). Timing of breakup and thermal evolution of a pre-Caledonian Neoproterozoic exhumed magma-rich rifted margin. *Tectonics*, *38*, 1843–1862. https://doi.org/10.1029/2018TC005375

Received 23 OCT 2018
Accepted 20 MAR 2019
Accepted article online 11 APR 2019
Published online 5 JUN 2019

Timing of Breakup and Thermal Evolution of a Pre-Caledonian Neoproterozoic Exhumed Magma-Rich Rifted Margin

Hans Jørgen Kjøll[1], Torgeir B. Andersen[1], Fernando Corfu[1], Loic Labrousse[2], Christian Tegner[3], Mohamed Mansour Abdelmalak[1], and Sverre Planke[1,4,5]

[1]The Centre for Earth Evolution and Dynamics, University of Oslo, Oslo, Norway, [2]Sorbonne Université, CNRS-INSU, Institut des Sciences de la Terre Paris, ISTeP UMR 7193, F-75005, Paris, France, [3]Centre of Earth System Petrology, Department of Geoscience, Aarhus University, Aarhus, Denmark, [4]Volcanic Basin Petroleum Research, Oslo Science Park, Oslo, Norway, [5]Research Centre for Arctic Petroleum Exploration (ARCEx), UiT The Arctic University of Norway, Tromsø, Norway

Abstract During the terminal stages of Wilson cycles, remnants of magma-poor margins may be incorporated into the orogens, whereas the magma-rich margins often are lost in subduction due to low buoyancy. The understanding of magma-rich margins is therefore mostly based on drill holes and geophysical observations. In this contribution, we explore the temporal evolution and the ambient conditions of a magma-rich rifted margin preserved within the Scandinavian Caledonides. The Scandinavian Dike Complex was emplaced into a sedimentary basin during the initial breakup and opening of the Iapetus Ocean 615 to 590 million years ago. The dike complex constitutes 70–90% of the magma-rich, syn-rift basins and is locally well preserved despite the complex Caledonian history. This contribution provides new observations about the geometry, relative timing, and development of the margin. Jadeite-in-clinopyroxene geothermobarometry, titanium-in-biotite geothermometry, and garnet isopleth modeling show that the ambient pressure and temperature conditions were similar for the entire dike complex at 0.25 to 0.45 GPa, with contact metamorphic temperatures up to approximately 700 °C. In the northernmost part of the study area, U-Pb dating of magmatic zircon shows that partial melting of the sedimentary host rock, at relatively shallow levels, occurred at 612 Ma. This shows that the crust was molten already 6 million years before the northernmost dike swarm was emplaced at 605.7 ± 1.8 Ma. We propose that the locally pervasive partial melting occurred due to high geothermal gradients and introduction of mafic melt in the lower crust. These processes significantly reduced the strength of the crust, eventually facilitating continental breakup.

Plain Language Summary This project investigates what the crust looks like and how it behaves when continents are rifting and finally break apart to form a new ocean. Sometimes the breakup is associated with magmatism. When this is the case the structure and behavior of the crust change dramatically from their state when no magma is involved. One important implication is that the heat brought by the magma presumably makes the crust very hot and weak and thus easier to break. Direct observations of magma-rich rifted margins are sparse, but in an area of Scandinavia, the deep parts of a rift in the Earth's crust have been preserved and exposed through complex geological processes. The study of these rocks reveals the processes that were active at depth when the continents broke apart. We have used mineral chemistry and age dating to show that the studied areas formed at approximately 9- to 16-km depth more than 600 million years ago. Our observations indicate that the stretching started when the crust was relatively cold, possibly causing earthquakes. Later, the crust was heated by magma intrusions to such a degree that it started to melt and became very weak, which made it easier to stretch and break the continent apart.

1. Introduction

Understanding the formation and evolution of passive margins is important because they provide clues as to how continents break apart and to constrain the transition from rifting to drifting in the divergent stages of the Wilson cycles (e.g., Brune, 2016; Buiter & Torsvik, 2014). Present-day rifted margins are generally submerged and buried like the northeast Atlantic (e.g., Clerc et al., 2018; Faleide et al., 2008; Gernigon et al.,

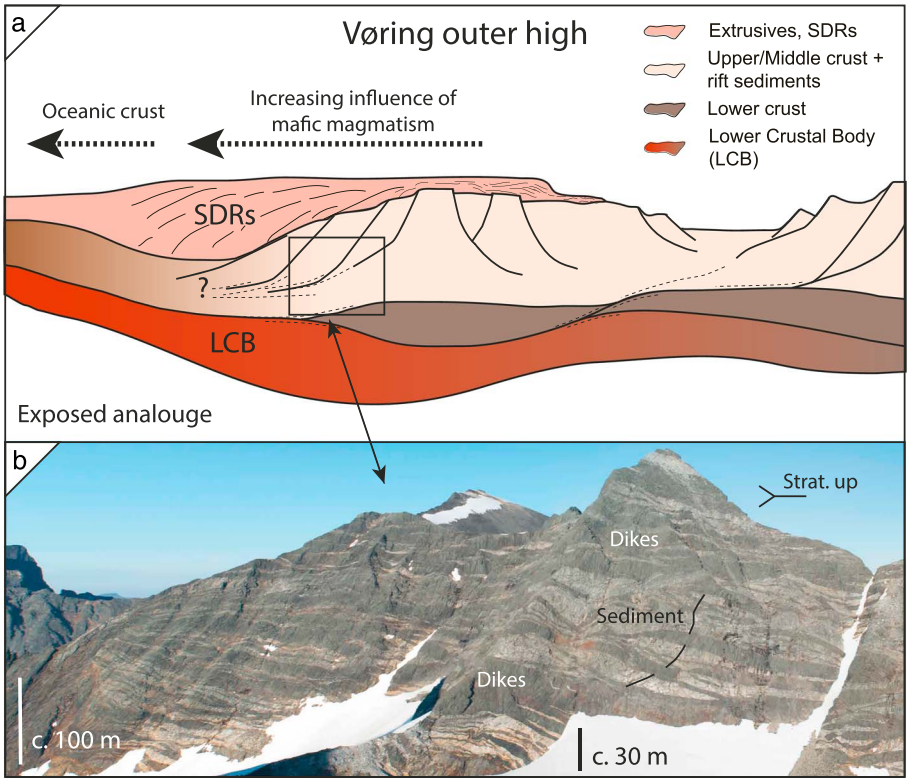

Figure 1. (a) Schematic illustration of a magma-rich margin, modified from Abdelmalak et al. (2017). Fossil analogue indicated by black rectangle. The fossil analogue is in an area with syn-rift sediments and originally vertical dikes. SDR = seaward dipping reflector sequence; LCB = lower crustal body. Dashed lines indicate ductile shear zones. (b) Oblique photograph of a cliff section in the southern segment showing the exposed analogue. Light-colored rocks are sediments (black lines indicate bedding), dark colored rocks are doleritic dikes. Bedding is subvertical and indicated by black lines. Dikes are subhorizontal. The entire area was tilted during the Caledonian orogeny and stratigraphic up is toward the right in the picture. The exposed cliff section is approximately 1 km long and approximately 250 m high.

2004) and only rarely exposed, like in the Afar rift (e.g., Bastow & Keir, 2011; Stab et al., 2016) or in the Gulf of California (e.g., van Wijk et al., 2018). Some fossil rifted margin analogues can be found in Phanerozoic mountain belts around the world like in the southern Scandinavian Caledonides (Andersen et al., 2012; Jakob et al., 2017), Appalachians (Chew & van Staal, 2014), Alps (Manatschal, 2004; Manatschal & Müntener, 2009; Mohn et al., 2014), and Pyrenees (Lagabrielle et al., 2010), but these are generally classified as magma-poor rifted margins. Their magma-rich counterparts, on the other hand, are often lost by subduction due to metamorphic densification. Exposed crustal sections of the magma-rich end-member are therefore much less known, and what we do know about their architecture mainly comes from geophysical methods and drill hole data (e.g., Direen & Crawford, 2003; Gernigon et al., 2004; Theissen-Krah et al., 2017; Zastrozhnov et al., 2018). In general, these magma-rich rifted margins show an anomalously thick ocean-continent transition (~20-km thickness), commonly referred to as the outer high (Figure 1). This area is generally characterized by three levels, which from top to bottom, are (1) major extrusive complexes represented by wedges of basaltic flows and tuffs, which are seismically imaged as seaward dipping reflectors (SDRs in Figure 1; Eldholm, 1991; Menzies et al., 2002; Planke et al., 2000); (2) dike and sill complexes within the upper and middle continental crust (Abdelmalak et al., 2015; Geoffroy et al., 2007; Klausen & Larsen, 2002); and (3) a lower crust of unknown composition, characterized by high seismic velocity (lower crustal body in Figure 1; Holbrook et al., 2001; Kelemen & Holbrook, 1995; White et al., 2008, 1987; Figure 1).

Although tectonic rifting generally precedes magmatism at rifted margins, anomalous magmatic productivity resulting from elevated mantle temperatures will significantly weaken the lithosphere and promote strain localization (Buiter & Torsvik, 2014). However, magma emplacement is commonly a very rapid

process. Its effect on the crustal rheology may be dual depending upon the duration of the magmatism: (1) thermal weakening, when newly formed hot intrusions are emplaced and heat their surroundings, and (2) rheological hardening, when mafic intrusions solidify and cool and thereby becoming more competent. Consequently, the localization of the deformation depends on the emplacement rate, volume, and spatial organization of the mafic system (Bialas et al., 2010; Daniels et al., 2014).

Understanding the relationship between rifting and magmatism in magma-rich margins requires additional constraints on melting conditions such as pressure, temperature, and melt fraction. Unraveling the age sequence of magmatic products is therefore essential to constrain magmatic productivity in time and space. These parameters are important to test and validate geodynamic scenarios and to improve input parameters for numerical models of magma-rich margins. Most of the present-day magma-rich margins are submerged offshore and are therefore difficult to study by direct observation.

The Scandinavian Dike Complex (SDC) in northern Scandinavia offers a unique chance to study an exhumed and thrusted ancient analogue of a magma-rich margin, permitting direct observation and sampling and thereby providing an improved understanding, particularly of the deeper crustal levels. In this contribution we report field observations from a section representing deep levels of the ocean-continent transition of a magma-rich rifted margin. The field areas are generally constituted by more than 70% mafic dikes, which intrude syn-rift sediments (Figure 1b). We use field observations coupled with U-Pb geochronology to investigate the temporal and spatial development of the rifted margin. Geothermobarometry of magmatic clinopyroxenes and contact metamorphic mineral assemblages, that escaped metamorphism related to Caledonian burial and nappe stacking, is used to estimate pressure and temperature at the time of dike crystallization and how these parameters have changed through time. These data suggest that the arrival of a heat pulse led to local widespread anatexis during continental stretching.

2. Geological Setting

The first evidence for an attempted opening of the Iapetus Ocean is represented by local magmatic events that occurred approximately 835 to 850 Ma (Paulsson & Andreasson, 2002; Walderhaug et al., 1999; Figure 2), but it was not until 200 million years later, in the Late Neoproterozoic, that Baltica and Laurentia finally rifted apart and the Iapetus Ocean opened. Before the opening, however, rift basins developed, and syn-rift sediments were deposited. These sediments consisted primarily of Neoproterozoic sandstone and shale overlain by a sequence of carbonate, which locally show evidence for evaporite deposits (Svenningsen, 1994b). Locally, the carbonate sequence is overlain by a diamictite unit, which again is overlain by thick clastic packages, comprised by up to several kilometers of shallow marine sandstone (Nystuen et al., 2008; Stølen, 1994; Svenningsen, 1994b; Zwaan & van Roermund, 1990).

During the breakup event, the SDC was emplaced along approximately 1,600 km of Baltican continental margin (e.g., Andréasson et al., 1992, 2018; Tegner et al., 2019). During this event the sediments were metamorphosed (for convenience the prefix "meta" is omitted from the rest of the text). Precise U-Pb zircon and baddeleyite ages of mafic dikes from various sites along the original margins of Iapetus vary from 616 to 595 Ma (e.g., Kamo et al., 1989; Bingen et al., 1998; Svenningsen, 2001; Ernst & Bell, 2010; Baird et al., 2014; Gee et al., 2016; Kumpulainen et al., 2016; this study, see section 3.1.3). The best preserved remnants of the allochthonous SDC crop out over an area covering roughly 6,000 km^2 and stretching for almost 900 km from 62.8°S in central Sweden to approximately 70°N in northern Norway (Figure 2). The southernmost exposure of the SDC, however, is the 616 ± 3 Ma Egersund dikes, which were emplaced in the autochthonous Baltican basement (Figure 2; Bingen et al., 1998). A recent compilation of the geochemistry of the SDC reveals a systematic zonation in trace element compositions with a geographically progressive δ-Nb and La/Sm enrichment (E-MORB) relative to mid-ocean ridge basalt, implying that the formation of the magma was associated with elevated temperatures at the lithosphere-asthenosphere boundary (Tegner et al., 2019).

The distal, magma-rich rift segment was affected by convergent plate motions both during early and late stages of the Caledonian-Appalachian mountain building, as interlayered metasedimentary rocks (marble, pelites, and thin-bedded quartzites) and pillow basalts and sills/dikes in the Seve nappe of northern Sweden were affected by Early Ordovician eclogite facies metamorphism at approximately 480 Ma (Kullerud et al., 1990; Root & Corfu, 2012; Figure 2). Final closure of Iapetus and continental collision

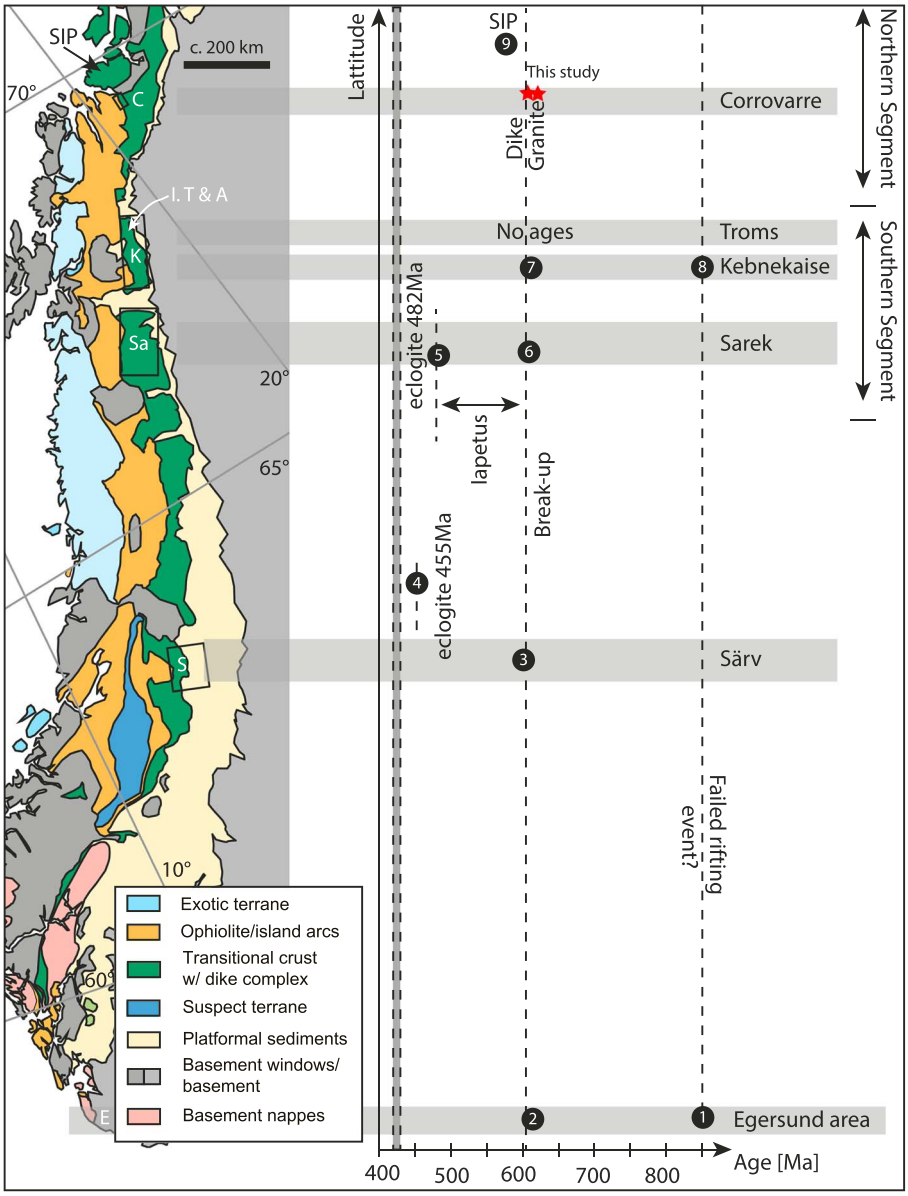

Figure 2. Simplified tectonic map of the Scandinavian Caledonides and timeline of the initial Caledonian Wilson Cycle. Field areas are indicated by black rectangles. E = Egersund, S = Särv, Sa = Sarek, K = Kebnekaise, I. T = Indre Troms, A = Abisko, C = Corrovarre, SIP = Seiland Igneous Province. Latitude versus age diagram displaying all major events from the proposed 850 Ma failed rifting event, through the successful rifting event at 600 Ma and finally closure of the Iapetus Ocean during Scandian collision. 1 = Hunnedalen dikes (Walderhaug et al., 1999), 2 = Egersund dikes (Bingen et al., 1998), 3 = Särv dikes (Kumpulainen et al., 2016), 4 = Jamtland eclogites (Majka et al., 2012), 5 = Tsäkkok eclogites (Root & Corfu, 2012), 6 = Sarek dikes (Svenningsen, 2001), 7 = Kebnekaise dikes (Baird et al., 2014), 8 = Vistas granite (Paulsson & Andreasson, 2002), 9 = Seiland Igneous Province (Roberts et al., 2010).

took place in the Middle Silurian (Figure 2; 430–425 Ma) and peaked at 410 ± 10 Ma during Caledonian "Scandian" continental collision (e.g., Corfu et al., 2014) when outer parts of the Baltican basement reached ultrahigh pressure conditions (e.g., Hacker et al., 2010; Smith, 1984). The magma-rich rifted margin was stacked in nappe complexes and transported more than 600 km onto Baltica and is now called the Seve Nappe Complex (Gee, 1975; Jakob et al., 2019). Most of the rocks underwent intense deformation and metamorphism, but there are kilometer-sized tectonic lenses of the SDC and their wall rocks that are little deformed and preserve the pre-Caledonian mineral assemblages. These lenses are

presently found as kilometer-sized tectonic lenses with gradational boundaries to intensely deformed counterparts and constitute the field area for this study.

3. Field Observations

This paper mainly focuses on the allochthonous dike complex from approximately 69.8°N in Corrovarre to approximately 67°N in Sarek but also presents paleo pressure data from approximately 63°N in Särv (Figure 2). The field areas have been subdivided in a northern and a southern segment and show well-exposed and well-preserved sections of densely dike-intruded sediments and basement (Figures 1 and 2).

As all the areas reside in nappes, absolute orientations of dikes and bedding are secondary and will not be discussed further. Relative angles, that is, angle between dike and bedding, will be reported and discussed. Internal shear zones within the nappes further complicate correlations; therefore, we are focusing on observations from large and well-exposed outcrops and avoid zones with obvious overprint of Scandian deformation and regional metamorphism.

3.1. Northern Segment

The least deformed parts of the northern segment cover an area of approximately 24 km^2 and consist largely of highly intruded sediments. The best preserved lens near Corrovarre (Figure 2) was mapped in detail by Zwaan and van Roermund (1990) and Lindahl et al. (2005).

3.1.1. Mafic Dike Complex and Contact Relationships

The mafic dike swarm at Corrovarre intrudes quartzite, marble, and arkose, with mica-rich horizons displaying the sedimentary layering in the clastic rocks (Figure 3a). The bedding is typically disrupted by shear bands indicating bedding-parallel stretching (Figure 4a). The mafic dikes form anastomosing networks with en echelon geometries covering approximately 50–70% of the area (Kjøll et al., 2019). Chilled margins are preserved. Locally, some dikes are vesicular where emplaced in carbonates. The geometry of the dikes is strongly controlled by the rheology of the sediments in which they intrude, for example, where they intrude carbonates they commonly have a short and stubby shape and apparent boudinage (Kjøll et al., 2019). Their tips, where visible, are blunt with sediments draping over the tip indicating that the dikes were emplaced in a forceful manner (Kjøll et al., 2019; Figures 3a and 3b).

3.1.2. Migmatization and Deformation

The sediments at Corrovarre show variable degrees of partial melting and are in general more affected by migmatization than in the southern segment, locally reaching diatexite textures. In some areas, pristine sediments can only be found in rafts floating in leucosome (Figure 4c). Asymmetric shear bands that record bedding-parallel stretching are common and show that the sediments were at suprasolidus conditions during the stretching stage (Figure 4a). Partial melting appears to have been contemporaneous with the stretching as leucosomes coalesce in the developing shear bands and, locally, granites intrude the stretched sediments (Figures 4c and 4d). Mafic dikes cut both the sediments and the granites (Figures 3a and 3c), although locally the granites and the mafic dikes also show evidence of mingling, suggesting that there are both pre- and syn-dolerite granites. Furthermore, mafic dikes with highly irregular and lobate boundaries to the host migmatite/sediment indicate that the migmatite was partially molten during mafic dike emplacement (Figure 4b). Locally, the leucosomes coalesce and form granite sheets (Figure 3c). These are cut and locally drag folded along margins of dolerites.

3.2. Southern Segment

The southern segment includes the areas of Sarek, Kebnekaise, Abisko, and Indre Troms and covers an area of approximately 1,660 km^2 (Figure 2). The dike complex in Sarek and Kebnekaise has yielded U-Pb zircon ages ranging from 608 to 578 Ma (Baird et al., 2014; Kirsch & Svenningsen, 2015; Svenningsen, 2001) and intrudes presumed late Neoproterozoic syn-rift sediments and basement (Kumpulainen & Nystuen, 1985; Nystuen et al., 2008). In the lower part of the stratigraphy, the sedimentary rocks also comprise a carbonate unit with local evaporite deposits (Spika Fm) overlain by thick-bedded sandstones, locally with more micaceous domains (cf. Favoritkammen Group, Svenningsen, 1994b; Figures 3d and 3e). In the upper part of the carbonates at Sarek, we recently discovered columnar stromatolites directly below a diamictite horizon that separates the carbonates and the sandstones. This may be a key horizon for correlation between the different basins in the SNC and other basins in the circum-Iapetus.

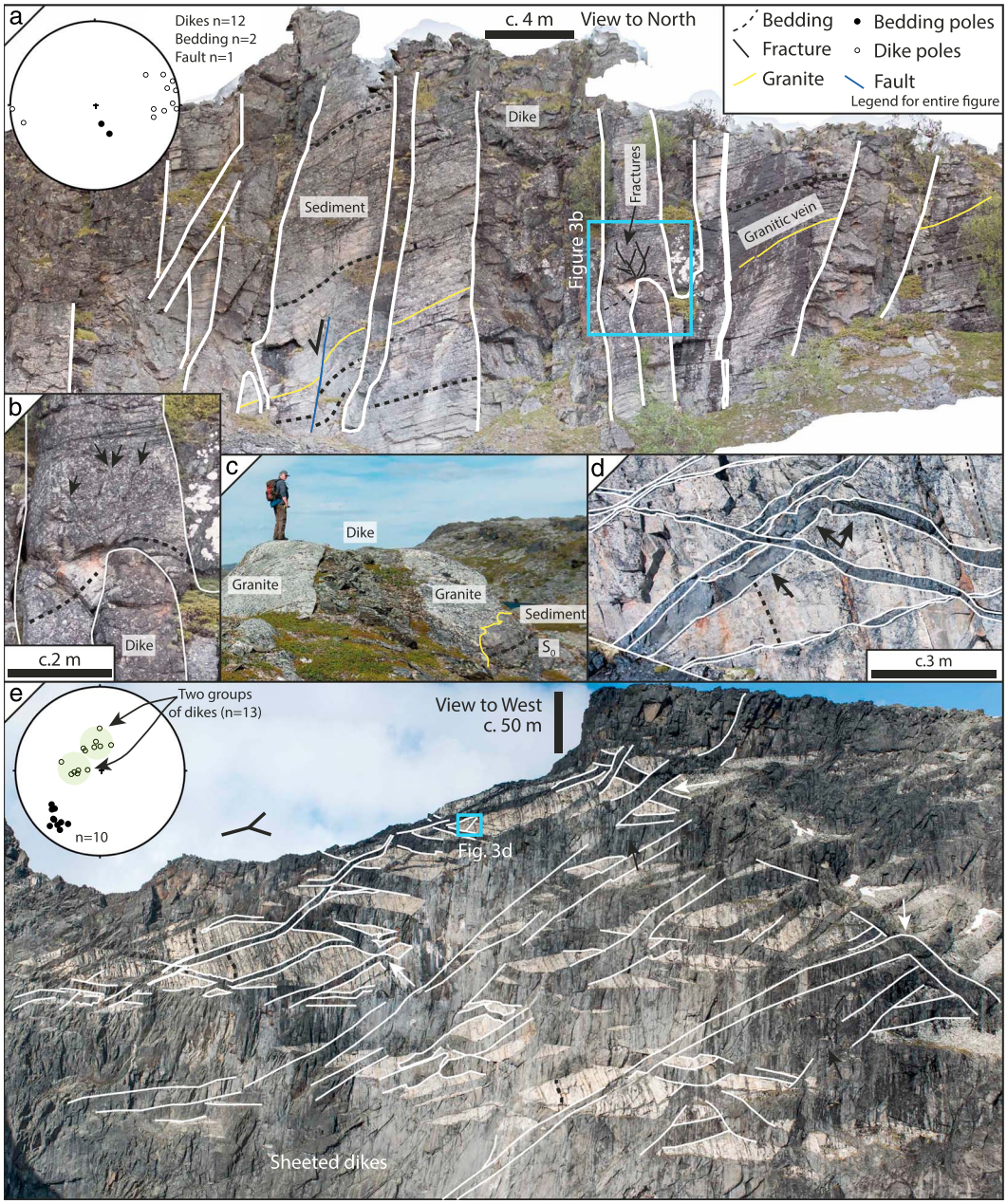

Figure 3. Overview figure showing dike geometries in large cliff walls. (a) Twelve-meter-tall cliff in Corrovarre with mafic dikes cutting already metamorphosed sediments and predike granite veins (yellow line) of unknown age. Stereonet shows poles of dikes (open circles) and bedding (closed circles). Locally, there are steep normal faults subparallel to the dikes. They also cut bedding and the thin granitic veins. (b) Close-up of a dike tip (black rectangle in Figure 3A); the termination is blunt, and the bedding is folded around the tip (dashed line), with fractures propagating into the arkosic host sandstone. (c) A mafic dike truncates a granite sheet in Corrovarre. The yellow line indicates the discordant contact between granite and host sandstone (see section 4.2 for geochronology of this granite). (d) Detail of Figure 3E from Sarek shows the complexities of the dike emplacement, where a dike, indicated with black arrows, display an abrupt change in orientation. Dashed line indicate bedding. (e) Part of a 300-m-high, vertical cliff from Sarek, which is composed of more than 80% mafic dikes (dark rocks, highlighted locally with white lines to indicate cross-cutting relationships). Some dikes show abrupt changes in orientation (white arrows). The dikes intrude arkosic sandstone (light colored rocks) with preserved but locally folded bedding (black dashed lines; see also the supporting information). Stereonet show poles of dikes (open circles) and bedding (closed circles. Note grouping of dike orientations, separated by a 30° angle. The entire sequence has been tilted and stratigraphic up is now toward left in the figure.

3.2.1. Dike Complex and Contact Metamorphism

Approximately 70% of the area consists of mafic dikes that intrude the more than 2.5-km-thick sedimentary pile (Svenningsen, 1994a). Dikes mainly form two groups separated by an angle of approximately 30°

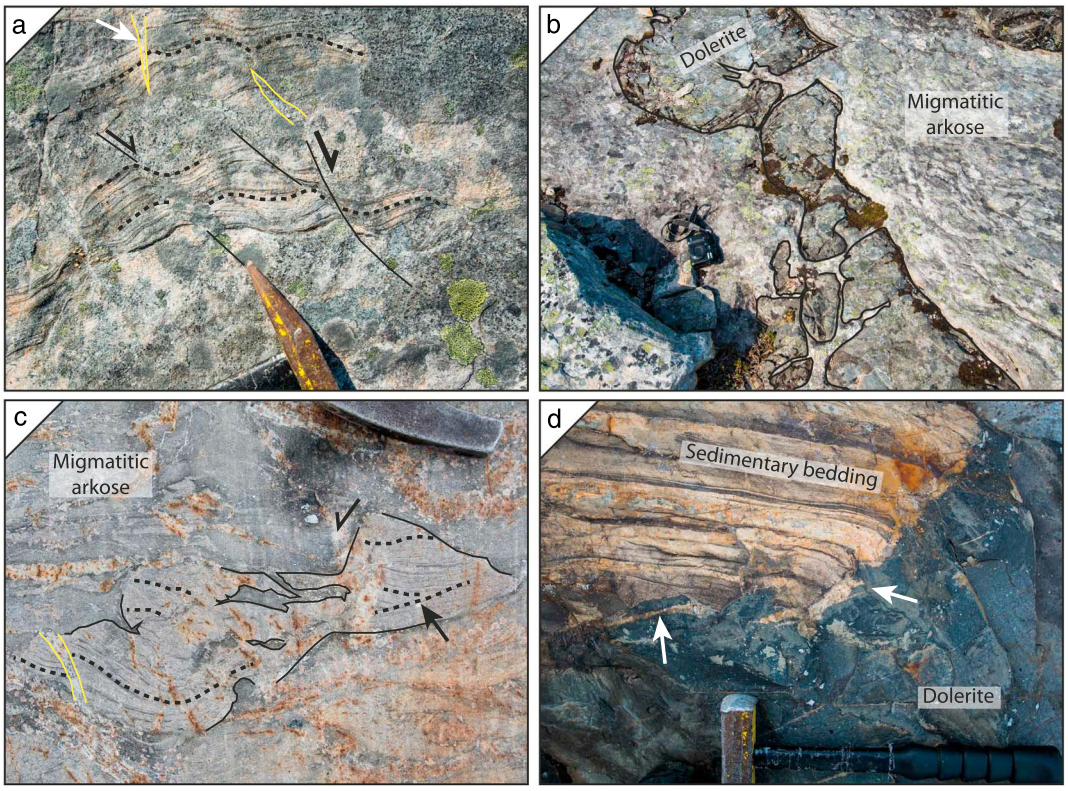

Figure 4. Overview plate showing evidence for migmatization of the host rock in the dike complex. (a) Deformed migmatitic arkosic sandstone in Corrovarre. Shear bands are highlighted by black lines and are locally filled with leucosomes (yellow lines and white arrow highlights a leucosome) indicating contemporaneous melting and deformation. Black dashed lines indicate bedding. (b) Dolerite intruded into partially molten arkose forms highly irregular and lobate boundaries to the host rock indicating that dike emplacement was contemporaneous with migmatization. Digital camera for scale. (c) Deformed and migmatitic arkosic sandstone from Indre Troms developed bedding-parallel stretching during anatexis. Bedding is highlighted with black dashed lines. Black arrow shows cross-bedding. The preserved sandstone is highlighted by black solid lines. Leucosome has segregated and coalesced in shear bands. Locally a thin granitic dike (highlighted by yellow lines) cut the bedding. (d) Mingling between dolerite and granite. The presence of leucosome at the contact with a sedimentary raft (white arrows), together with the back veining in the dolerite and irregular contacts of the raft suggest contact metamorphic melting of the sediment during dike emplacement.

(Figure 3e), but bent geometries are also common (Figure 3d). Mutually cross-cutting relationships between these two orientations suggest contemporaneous emplacement (Kjøll et al., 2019; Figures 3d and 3e). At a larger scale (hundreds of meters) the dikes form an anastomosing network as seen for example in a 1.5-km-long continuous cliff exposure of the dike complex (Kjøll et al., 2019; Figure 3e and the supporting information). Features such as chilled margins, dike apophyses, and bridges are common.

Most of the host sediments have been metamorphosed into hornfels without cleavage. Locally contact metamorphic mineral assemblages are preserved in the more micaceous domains, where dendritic to hopper-type garnets have grown together with andalusite (chiastolite), which has been pseudomorphosed into sillimanite (see section 5.3). At lower levels in the stratigraphy, chlorine-rich scapolite ($Me_{45\text{-}50}$) is commonly present along margins and as veins along fractures in the dolerites and in the matrix of the sediments. It is derived from metasomatic alteration sourced from the evaporitic horizons (Svenningsen, 1994b). Locally, both sediments and thin mafic dikes are completely metasomatized into calc-silicates with grt + scp + di (the contact metamorphism is quantified in section 5, below; mineral abbreviations are from Whitney & Evans, 2010).

3.2.2. Partial Melting and Deformation

Variable partial melting textures are observed throughout the southern segment. In Indre Troms melting was locally pervasive forming metatexites with up to 10% leucosome (Figure 4c). Locally, the melt back veined the dolerites, especially where partial melting of the host sediments was pervasive (Figure 4d). In the south, the migmatization was less pervasive with leucosome pockets only found at contacts between dikes and sediments (Figure 4d). Leucosome pockets derived from the sediments are observed especially

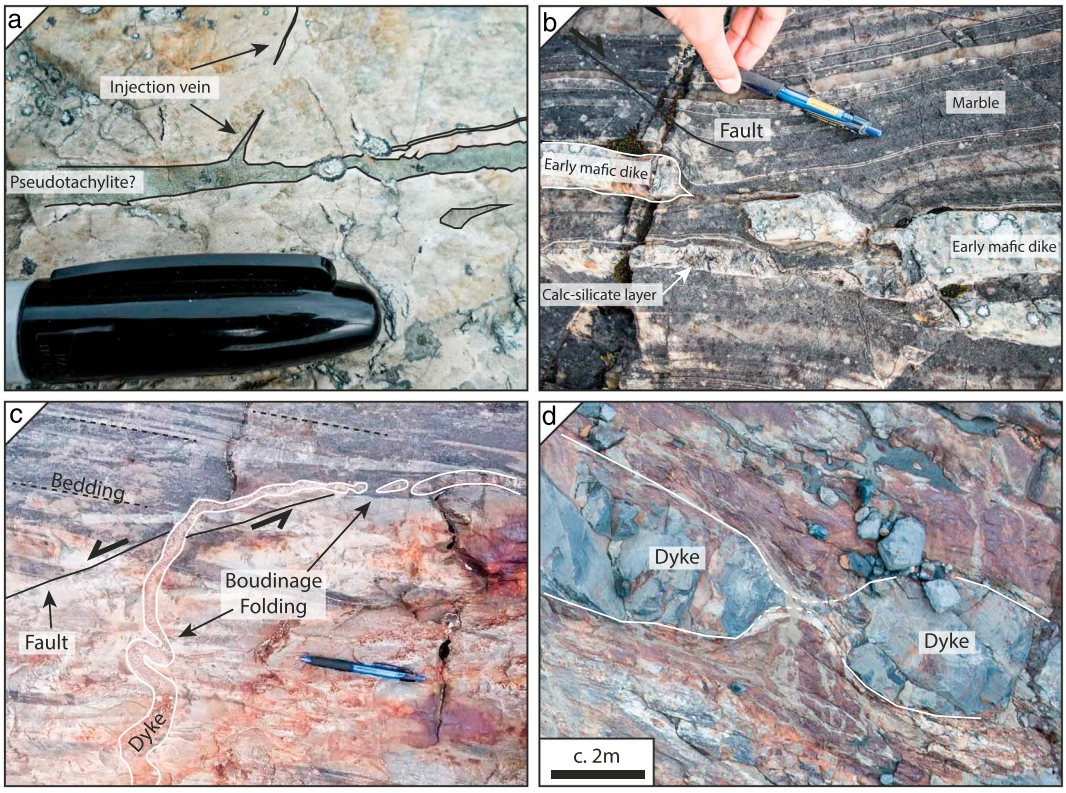

Figure 5. Overview figure showing bedding-parallel stretching in the same area but by different mechanisms. (a) injection veins of very fine-grained material, presumably recrystallized pseudotachylite or ultracataclasite, into homogenous sandstone. (b) Early mafic dike (early with respect to the main dike emplacement) and calc-silicate layers defining bedding in a marble, being cut asymmetrically by shear bands (black line). The color of the dike is caused by surface oxidation. (c) Thin dike cutting a low-angle normal fault (black line; inclined with respect to the bedding) in a sandstone. The dike is bent above the normal fault and the upper part parallel to the fault is boudinaged, whereas the lower part, at an apparent angle of approximately 60° to the normal fault, is folded. All three deformational features are compatible with bedding-parallel stretching and bedding-normal shortening. (d) Symmetric boudinage of an approximately 2-m-thick dike (highlighted by white lines).

close to dike terminations where the dikes are organized in an en echelon configuration with bridges both intact and broken (Figure 4d). Domains with no partial melting are also common, especially in the southernmost part of the segment.

The earliest deformation recorded in the southern segment is a progressive bedding-parallel stretching of the sediments. Where partial melting of the host sediments associated with dike emplacement was pervasive, the bedding-parallel stretching is recorded in the migmatites as asymmetric boudinage with outcrop-scale shear bands (Figure 4c). Where the migmatization was less pervasive and concentrated at the dike contacts, leucosomes are intrusive into the dolerites (Figure 4d). Early phases of bedding-parallel stretching have been preserved in the sediments as >50-m displacements along low-angle normal faults locally decorated by extremely fine-grained material forming injection veins into the undisturbed host sandstones (Figure 5a). In the weaker carbonate layers the bedding-parallel stretching is accommodated by outcrop-scale shear bands deforming thin, early mafic dikes along asymmetric shear bands (Figure 5b). At one location in the sandstone dominated areas, a dike cutting a normal fault is bent and stretched in the upper part, parallel to the normal fault, but is shortened (folded) where the dike lies at a higher angle to the normal fault (Figure 5c). On a larger scale, in the same area, thicker dikes have been boudinaged. In the boudin necks the dikes are partially amphibolitized, but in the undeformed parts, they retain primary magmatic mineral assemblages (Figure 5d).

3.3. Särv

The Ottfjället mafic dike swarm intrudes a >4.5-km-thick sequence of late Neoproterozoic syn-rift siliciclastic sediments, comprising well-bedded quartzitic to arkosic sandstone verlain by calcareous deposits and a

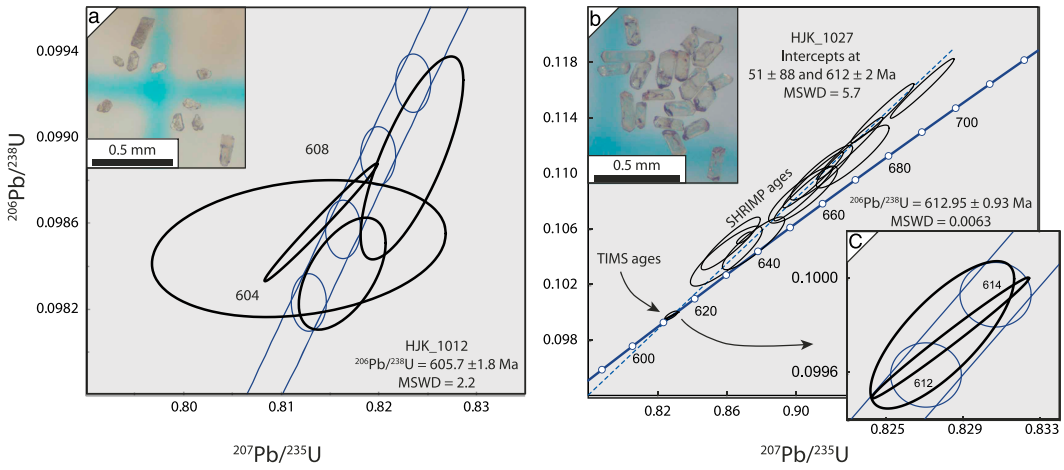

Figure 6. Geochronological data of zircon in a dolerite dike and a granite from Corrovarre. (a) Concordia diagram with data for four zircons from a medium-grained mafic dike. (b) Zircon data for a granitic sheet. The Sensitive High-Resolution Ion Micro Probe (SHRIMP) analyses yield reversely discordant data, presumably due to a matrix effect related to the high uranium content. A line fitted through the SHRIMP data intercepts the Concordia at 612 ± 2 Ma. (C) Two zircon grains from the same sample, dated using Chemical Abrasion Isotope Dilution Thermal Ionization Mass Spectrometer, yield concordant data with a $^{206}Pb/^{238}U$ average at 612.95 ± 0.93 Ma.

tillite/diamictite unit. These sediments are again overlain by clastic rocks and conglomerates (e.g., Gee, 1975; Hollocher et al., 2007; Kumpulainen, 1980).

Generally, the dikes and the bedding are near orthogonal. One direction dominates the dike orientation, but cross-cutting dikes also appear. The dikes are locally rotated by Caledonian ramp structures (Gilotti & Kumpulainen, 1986). The geometry of the dikes suggests en echelon formation with straight and sharp margins without cataclastic contacts to the host rock. The sandstone has a hard hornfels texture at the contacts changing to a primary sedimentary clastic texture further away. There is no evidence for either regional or local partial melting of the host sediment. The mafic dikes are generally well preserved and commonly contain fresh olivine together with clinopyroxene and plagioclase. The matrix has clinopyroxene and plagioclase as the main minerals and Fe-Ti oxides as accessory minerals. Although allochthonous, no penetrative Scandian deformation has been observed. Recent U-Pb dating of baddeleyite gives an age of 596 Ma for the dike complex (Kumpulainen et al., 2016).

4. Geochronology From the Northern Segment

Dolerites from the Corrovarre lens have previously been dated by Rb-Sr and Sm-Nd on minerals and whole rocks at 578 ± 64 Ma and 582 ± 30 Ma, respectively (Zwaan & van Roermund, 1990). Granite from the same lens was dated with U-Pb in zircon at 610.2 ± 1.1 Ma (Gee et al., 2016). In this study we have obtained new U-Pb ages for granite and dolerite using the sensitive high-resolution ion microprobe (SHRIMP) at Curtin University (see the supporting information) and chemical abrasion isotope dilution thermal ionization mass spectrometer (CA-ID-TIMS) at the University of Oslo. The latter follows the analytical procedures described in Corfu (2004) with additional information given in the supporting information.

4.1. Dolerite Dike

A medium-grained dike with subophitic texture has plagioclase and clinopyroxene preserving magmatic zonation. The 10 zircons found in the crushed sample were equidimensional fragments with diameters >50 μm (Figure 6a). The fragments were clear with some yellow-brown patches and often some crystal faces preserved, testifying to a euhedral growth of the zircon. Some euhedral grains were also found. These can be divided in two categories: (1) high aspect ratio (>2) and dark, brown color and (2) low aspect ratio (<2) clear, double terminated crystals (Figure 6a).

Four zircon fragments were selected based on clarity, lack of inclusions, and crystal shape and dated by CA-ID-TIMS, yielding an average $^{206}Pb/^{238}U$ age of 605.7 ± 1.8 Ma (Table 1; Figure 6a).

Table 1
Analytical Isotope Dilution Thermal Ionization Mass Spectrometer Data From Two Corrovarre Samples

Sample #	Weight (μg)	U (ppm)	Th/U[a]	Pb_c (pg)[b]	Isotopic ratios							Calculated ages				
					$^{206}Pb_c/^{204}Pb$[c]	$^{207}Pb/^{235}U$[d]	2σ (%)	$^{206}Pb/^{238}U$[d]	2σ (%)	ρ	$^{207}Pb/^{206}Pb$[e]	2σ (abs)	$^{207}Pb/^{235}U$[e]	2σ (abs)	$^{206}Pb/^{238}U$[e]	2σ (abs)	D[f]
HJK_1012	<1	300	1.8	1.2	1,515.7	0.816	0.4458	0.098	0.2166	0.55	607.6	8.1	603.6	2.0	604.8	1.3	0.5
HJK_1012	1	255	2.5	0.9	1,810.4	0.823	0.5255	0.099	0.3905	0.76	614.8	7.3	609.9	2.4	607.9	2.3	1.1
HJK_1012	<1	141	2.2	0.8	1,093.6	0.814	0.5802	0.099	0.2307	0.99	596.6	11.2	604.7	2.6	606.2	1.3	1.6
HJK_1012	<1	100	2.4	1.6	390.6	0.812	1.5167	0.098	0.2646	0.22	593.2	32.1	603.4	6.9	605.5	1.5	−2.1
HJK_1027	<1	964	0.1	2.1	2,801.4	0.828	0.3673	0.100	0.2565	0.76	608.0	5.2	612.5	1.7	613.0	1.5	−0.8
HJK_1027	<1	479	0.1	0.4	6,689.4	0.828	0.4019	0.100	0.2106	0.99	609.4	7.2	612.7	1.8	612.9	1.2	−0.6

Note. Coordinates for sample HJK_1012: 21°38′38.17″E, 69°50′0.698″N. Coordinates for sample HJK_1027: 21°40′6.174″E, 69°49′38.708″N.
[a]Model value calculated using $^{208}Pb/^{206}Pb$ ratio and the age of zircon. [b]Total common lead including blank and initial. [c]Corrected for spike contribution and fractionation. [d]Corrected for fractionation, spike and common lead, both blank and initial. [e]Corrected for fractionation, spike and common lead, both initial and blank. [f]Degree of discordance using $^{206}Pb/^{238}U$ and $^{207}Pb/^{206}Pb$ ratios.

4.2. Granites

A granite consisting of Qz + Plag + Kfs + Bt + Ms forms a sheet subparallel to the bedding, truncated by dolerites of the SDC, that is, a predike emplacement granite (Figure 3c). The sample contained abundant zircon grains that in general are clear and euhedral (Figure 6b). The zircons are often flat and plate like with an aspect ratio of the zircons varying from very high, >3 to <2. Growth zonation can be discerned even under the binocular microscope. The SHRIMP analyses plot reversely discordant (Figure 6b), probably due to a matrix effect caused by high levels of uranium (up to 11.800 ppm; White & Ireland, 2012) but may also have been affected by U-Pb perturbations. Therefore, an attempt was made to date the zircon grains using CA-ID-TIMS. After chemical abrasion, however, only two zircon fragments were left. They yielded two overlapping concordant analyses with an average $^{206}Pb/^{238}U$ age of 612.95 ± 0.93 Ma (Figure 6b). This age is identical within error to the average $^{207}Pb/^{206}Pb$ age of the SHRIMP data.

5. Mineral Chemistry and Geothermobarometry

Pressure and temperature are important factors that affect the geometries of a dike swarm as they control fracture mechanisms (e.g. Weinberg & Regenauer-Lieb, 2010). The Scandian thrusting of the SDC has caused rotations, and in most sections the sedimentary bedding is now steeply dipping to vertical (Figure 3e). In addition, the structural tops and bases, and even some internal domains of the observed sections, have secondary shear zone boundaries. Therefore, the depth of intrusion must be estimated by other methods than direct thickness measurements. We have already described the wall rocks as contact metamorphic with variable degree of partial melting and variably overprinted by regional Caledonian metamorphism. Here, we distinguish the various generations of metamorphic mineral assemblages and apply several geobarometers to the contact metamorphic paragenesis in the best preserved areas of the dike swarm to determine *PT* conditions during emplacement.

5.1. Dike Petrography

Texturally, the dolerites vary from porphyritic, with cpx ± plag ± ol as phenocrysts, to aphanitic with a matrix of cpx + opx + plag + opaques (Figure 7a). The most pristine mineral compositions are plagioclase (average: $Ab_{43} - An_{57} - Or_{0\text{-}1}$), pyroxene (average: $Wo_{39} - En_{46} - Fs_{13}$), and ±olivine (average: Fo_{82}) + Fe-Ti oxides ± scapolite (average: $Me_{43} - Mi_{50} - Si_7$) ± Qz ± Amp ± Bt. Plagioclase is zoned with An-rich cores. Within some of the clinopyroxenes a pervasive exsolution presumably of Fe-Ti oxides is present as thin (ø = ~1 μm) needles following crystallographic planes (Figure 7b). Most samples also show exsolution between clinopyroxene and orthopyroxene to varying degrees (Figure 7b). Electron microprobe analysis of the cpx crystals suitable for the pressure estimate (see below) display relatively homogeneous Al_2O_3 and CaO content (Figures 8a and 8b). The Sarek analyses show a weak trend with Al_2O_3 increasing and CaO decreasing with Mg#. For Na_2O most analyses are <0.35 wt%, except for Kebnekaise and five analyses from Sarek, which plot around 0.5 wt%. Kebnekaise analyses are clearly distinct from those from other localities (Figure 8b).

5.2. Magmatic Clinopyroxene Geobarometry

Crystallization pressures (Figure 9a) were estimated using the jadeite-in-clinopyroxene-liquid (jd-in-cpx-liq) geobarometer from Neave and Putirka (2017), and crystallization temperatures (Figure 9a) were estimated using equation 33 in Putirka (2008) as suggested in Neave and Putirka (2017). The jd-in-cpx-liq geobarometer is based on the pressure-dependent incorporation of jadeite, the Na component in clinopyroxene crystallized in equilibrium with basaltic liquid. The electron microprobe analysis data were filtered and checked for equilibrium with the whole-rock composition (Figures 9b and 9e) of the chilled margins as a proxy for the liquid composition. The strict filtering parameters suggested by Neave and Putirka (2017) reduced the number of cpx analyses from a total of 325 to 56, which were suitable for crystallization pressure and temperature determination (Figure 9; supporting information). Similar results are

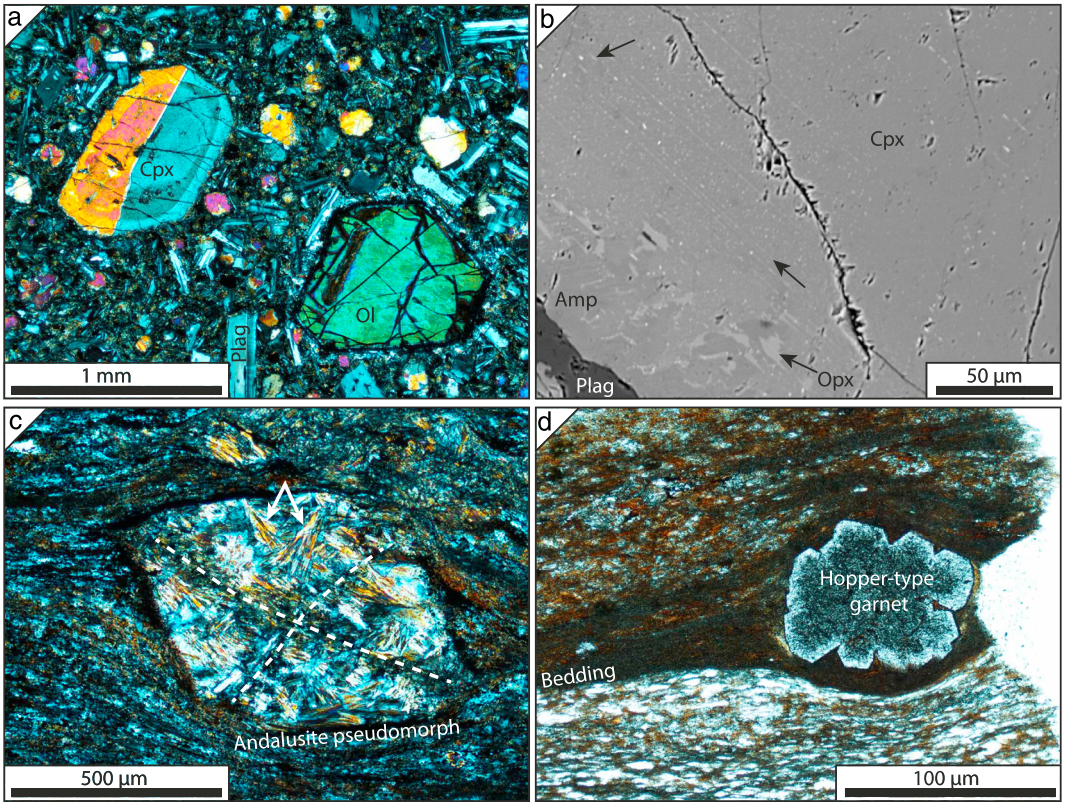

Figure 7. Overview of characteristic petrography. (a) Photomicrograph of a porphyric dolerite with phenocrysts of cpx, ol, and plag in a groundmass of cpx, plag, and opaques, mainly Fe-Ti oxides. (b) Backscatter electron image of a cpx crystal with approximately 1- to 5-µm-thick exsolutions of Fe-Ti oxides (arrow) and exsolved opx (lighter phase) in the rim (bottom left). (c) Photomicrograph of a chiastolite pseudomorph in a contact metamorphic fine-grained argillaceous sediment. The andalusite is completely replaced by fibrous sillimanite. (d) A hopper-type garnet, indicating rapid growth (Jamtveit & Andersen, 1992), in a biotite-rich horizon of an argillaceous sediment. The garnet has a thin (<10 µm) rim with less abundant inclusions of quartz and biotite.

also obtained when using more lenient filtering methods. More details of the procedure and the filtering criteria can be found in the supporting information.

The crystallization pressure calculations are summarized in Figure 9a. Results show some variation between different field areas. The southern segment is inhomogeneous with Sarek at 0.45 ± 0.04 GPa, Kebnekaise at 0.35 ± 0.04 GPa, and Troms at 0.25 ± 0.11 GPa. It should be noted that for Troms only two cpx analyses (out of 28) fulfilled the criteria of the geothermobarometer as given in Neave and Putirka (2017). Corrovarre, in the northern segment, yields 0.28 ± 0.11 GPa and Särv in the south 0.29 ± 0.06 GPa.

Calculations of the crystallization temperatures were based on the same filtered analyses as for the geobarometer and yield similar temperatures for all the field areas (Table 2). The temperature estimates are relatively homogenous and agree within 18 °C, with 1161 and 1179 as the extreme values, for the four different field areas. A positive correlation is observed between *T* and *P* estimates (Figure 9a).

5.3. Host Rock Petrography

The most common clastic sediments are quartzite, arkose, and greywacke and contain varying amounts of Qz + Fsp + Grt + Bt + Sil ± Ms ± Scp ± Ttn ± Ap ± Tur ± Zr. Carbonate, with bedding defined by calc-silicate layers, are generally found in the lower parts of the stratigraphy. In the least deformed parts, the sediments have a hornfels texture, generally without cleavage. Locally, and especially where the rock is rich in mica, millimeter-sized pseudomorphs of andalusite are statically recrystallized into fibrous sillimanite, without any preferred mineral orientation. The characteristic chiastolite habitus are commonly preserved (Figure 7c). Where the host rock consists of arkose and greywacke the more mica-rich domains often contain hopper- to dendritic-shaped garnets rich in inclusions as well as fibrous sillimanite (Figure 7d). Biotite has commonly overgrown the bedding in random directions.

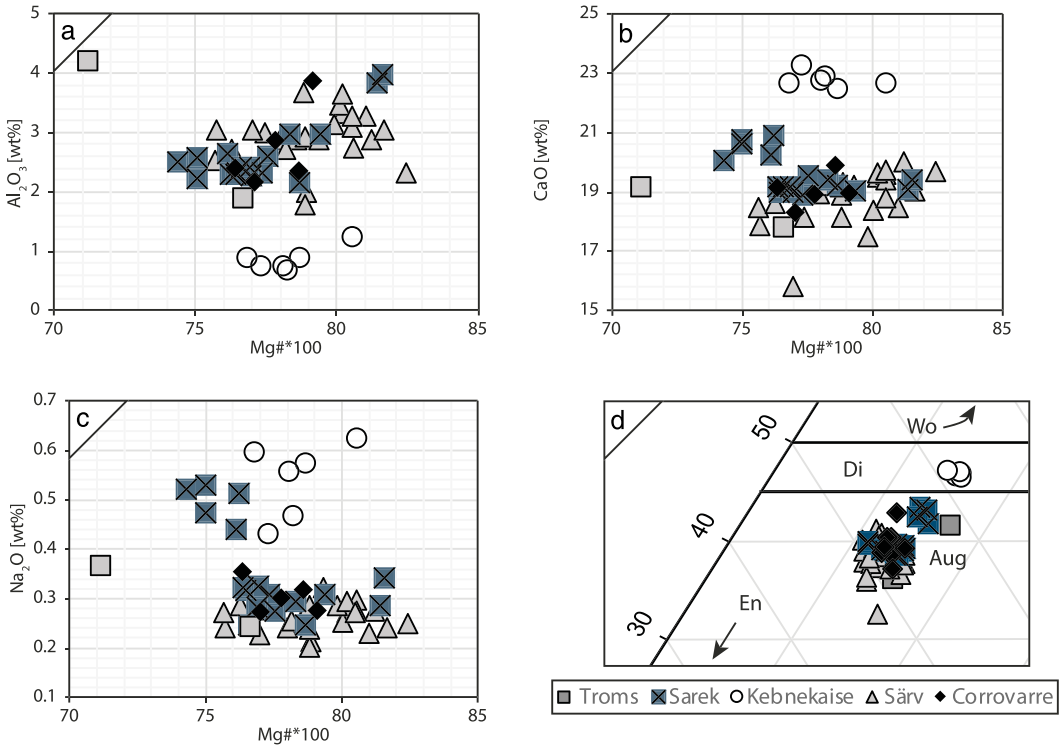

Figure 8. Clinopyroxene geochemistry (A–C) Major element chemical compositions of clinopyroxene plotted against Mg# of the clinopyroxenes. (D) Zoom in of the pyroxene triangular diagram. Note that the Kebnekaise samples all have magmatic diopside rather than augite and thus plot away from the other analyses.

5.4. *PT* Estimates From Pseudosection Modeling

Where the dikes intrude argillaceous sediments several pressure and temperature sensitive minerals have grown and can be used to deduce the metamorphic history of the rock. The garnets are generally unzoned and poikilitic and grew in the millimeter-thick mica-rich horizons that define the bedding in the sediment (e.g., Figure 7d). In general, the garnets are almandine rich (Alm_{70}), except for one sample, which is more grossular rich (Alm_{40}, Grs_{25}). The spessartine and pyrope contents are similar for all samples ($Prp_{10\ to\ 19}$). Most of the samples have sillimanite as very fine-grained fibrolite and, as previously mentioned, andalusite pseudomorphed by static growth of sillimanite, suggesting a prograde pressure and/or temperature path from the earliest to late stages of static growth (Figure 7c). Both biotite and muscovite also occur as neoblasts.

Calculation of almandine, grossular, pyrope, and spessartine garnet endmember isopleths (Theriak-Domino; de Capitani & Petrakakis, 2010) on a sample from Indre Troms (Figure 2) was used to estimate the ambient conditions during contact metamorphism. The sample is a mica-rich arkose sampled approximately 3 m from a fresh, approximately 5-m-thick dolerite dike. The pressures range from 0.25 to 0.35 GPa, and temperatures are 675–725 °C.

5.5. Ti-in-Biotite Geothermometry

Titanium in biotite geothermometry (Engel & Engel, 1960; Henry et al., 2005) has been applied on sediments containing biotite from Sarek and Indre Troms (Figure 2). The samples used for these analyses were collected approximately 1–5 m away from the dikes. The biotite used for the geothermometry shows subhedral to euhedral crystal shapes. To avoid complications due to multiple metamorphic events and secondary alteration processes, only analyses of biotite with random orientations (i.e., static growth) were used to calculate the contact metamorphic temperatures. Furthermore, analyses that indicate incipient alteration of biotite to chlorite were disregarded. The biotite analyses used in the temperature calculation had an average Mg# of 43 and average TiO_2 of 3.1 wt% (see the supporting information). The Ti-in-biotite

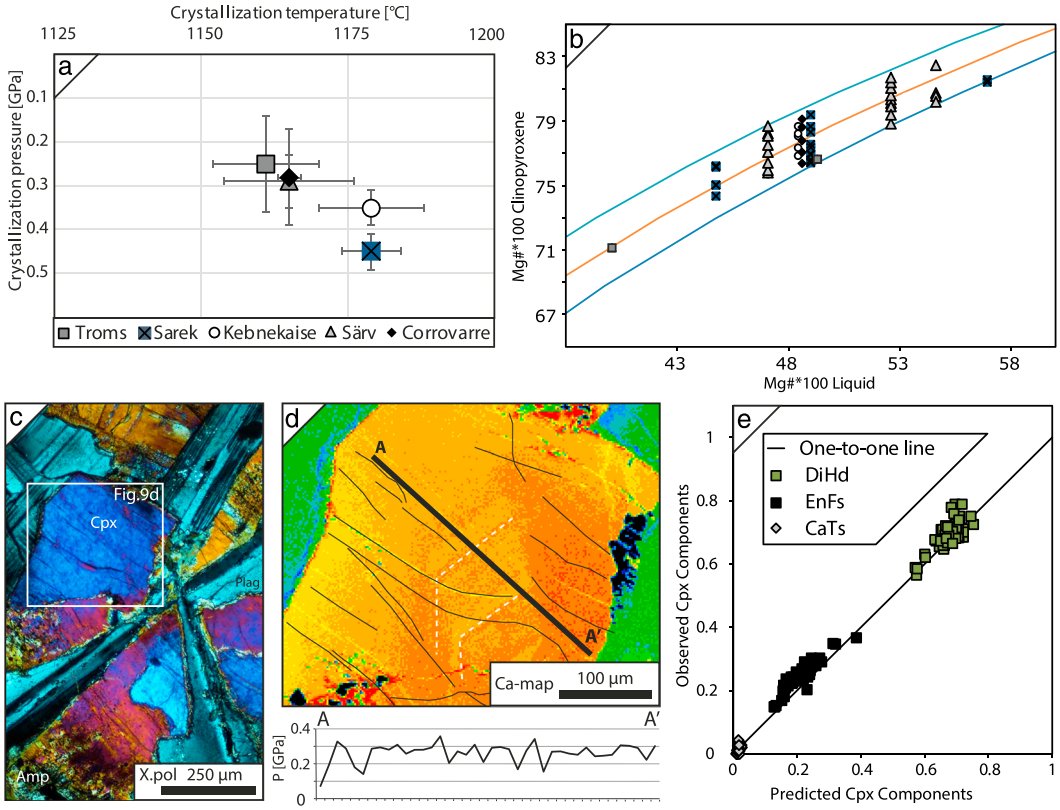

Figure 9. Overview of the crystallization pressure and temperature estimates. (a) Average crystallization temperature versus average crystallization pressure of the clinopyroxene. (b) Rhodes diagram checking equilibrium between cpx composition and "liquid," which in this case is assumed to be the whole-rock composition of the chilled margin of the dike (Putirka, 2008). Plot shows a selected K_D value of 0.27 (orange line) ± 0.03 for Fe-Mg in Cpx-liquid pairs. (c) Photomicrograph (crossed polarizers) of an analyzed magmatic cpx crystal from Corrovarre. (d) CaO, EMPA map of the cpx crystal in (c) shows magmatic zonation (white dashed lines) in the crystal. Thin black lines outline cracks seen on BSE image. Graph below the map shows *P* estimates along profile A-A′. (e) Observed and predicted cpx components used to calculate the crystallization *PT* conditions of the cpx.

geothermometer yields crystallization temperature of 693 ± 14 °C at Sarek, 713 ± 3 °C for Kebnekaise, 696 ± 19 °C and for Indre Troms 634 ± 6 °C (errors are 1σ).

6. Discussion

The rocks investigated in this study have undergone multiple metamorphic events. The first event, considered in this contribution, reflects the contact metamorphic heating by mafic intrusions emplaced at the distal margin of the Iapetus. The second event, that is, the orogenic event, is more frequently studied in the literature but also more complex and reflect the changing pressures and thermal imprint of the burial and

Table 2
Results From PT Estimates Using jd-in-cpx-liq Geothermobarometry From Neave and Putirka (2017) and the Geothermometer Ti-in-Bt From Henry et al. (2005)

	Crystallization pressure		Crystallization temperature		Avg. *T* from Ti-in-Bt	Error (1σ)	
Area	*P* (GPa)	1σ (GPa)	*T* (°C)	1σ	*T* (°C)	1σ	#Samples/ #analysis
Särv	0.29	0.06	1165	11	—	—	—
Sarek	0.45	0.04	1179	5	693	14	6/50
Kebnekaise	0.35	0.04	1179	9	713	3	1/7
Troms	0.25	0.11	1161	9	696	19	2/15
Corrovarre	0.28	0.11	1165	2	—	—	—

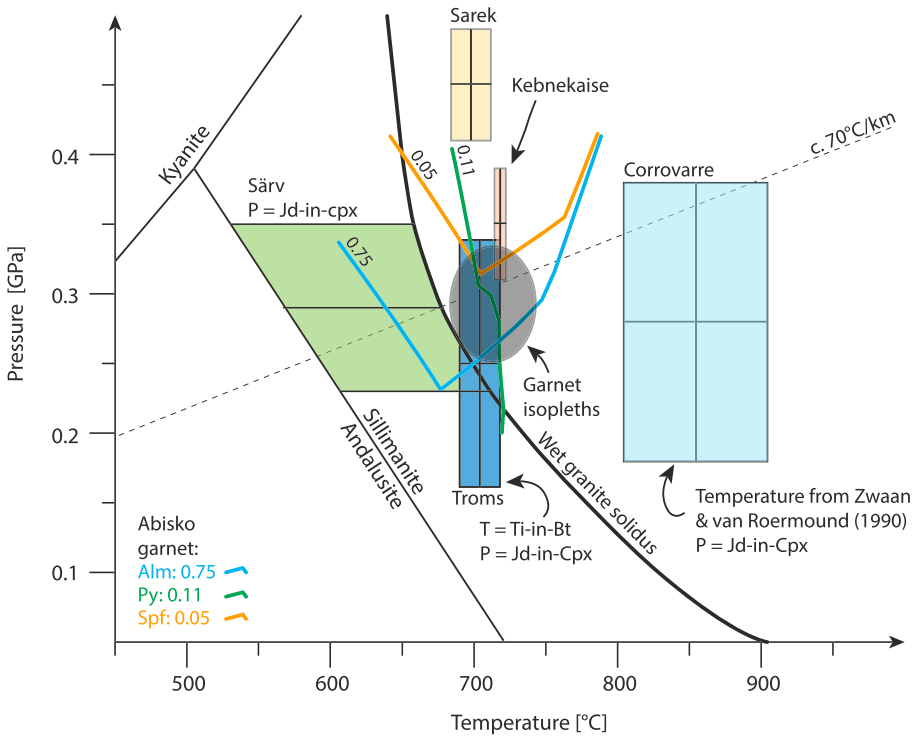

Figure 10. Summary of *PT* data from various geobarometers and geothermometers as well as garnet isopleths (blue, green and orange lines). Wet granite solidus is from Huang and Wyllie (1981), while the temperature estimate for Corrovarre is from Zwaan and van Roermund (1990).

subsequent nappe emplacement of the distal margin. Locally, this event reached eclogite facies conditions, although (garnet) amphibolite facies is more common. Shear zones cross-cutting all emplacement-related structures have amphibolite facies mineral assemblages. In summary, the first contact metamorphism was a high-temperature, low-pressure event, whereas the second, Caledonian event reached a diversity of metamorphic conditions (not discussed in detail here) but in general producing higher pressure mineral assemblages.

6.1. Ambient Conditions During Dike Emplacement

In the studied areas, the crystallization pressure estimates from the jd-in-cpx-liq geothermobarometer vary from 0.25 to 0.45 GPa, indicating a depth ranging from 9 and 16 km. Contact metamorphic temperatures estimated using Ti-in-Bt (Henry et al., 2005; Figure 10) are as high as 693 to 713 °C. This is also in agreement with contact metamorphic garnet isopleth calculations from Theriak-Domino modeling, which suggest temperatures ranging from 700 to 750 °C (Figure 10). The sediments sampled for geothermometry were collected 1 to 5 m from the dike contacts at different sites. They were originally sampled for detrital zircon geochronology; therefore, no profiles away from a dike have been sampled. The temperature estimates are therefore limited to one specific spot at varying distances to the dikes. All sample sites are highly intruded (>70% by volume) by dikes. As such we believe that the calculated temperature is a good estimate of the ambient thermal conditions of the area. We cannot, however, assess how much magma flowed through the conduit and for how long. This would presumably have an effect on the temperature of the host rock as the temperature of the host, at a specific point away from the dike, would increase with increasing flow. Such prolonged flow may have caused the higher degrees of partial melting that we observe in Indre Troms, Corrovarre, and to a certain degree Sarek. The field observations presented above show that the pressure-temperature conditions for the contact metamorphism estimated here are above the solidus for partial melting of water-rich arkoses with a granitic mineralogy at ~660 °C at 0.3 GPa (e.g., Clemens & Holness, 2000; Johannes, 1984). No samples suitable for Ti-in-Bt were collected from Corrovarre, but Zwaan and

van Roermund (1990) using a leucosome containing two pyroxenes obtained a temperature of 850 ± 50 °C, significantly higher than what has been shown for the other areas to the south.

Field observations from the southern segment of the SDC show a progressive evolution of the strain accommodation mechanisms (brittle to ductile) as the temperature increased. In the southern segment, some early faults are decorated by recrystallized pseudotachylite veins (Figure 5a). These faults are cut by mafic dikes, which are themselves deformed by ductile mechanisms. The orientation and kinematics of these structures can be explained by a single stress system, resulting in stretching in the long limb and shortening in the short limb of the bent dike. Furthermore, the normal fault truncated by the dike is also favorably oriented within such a stress field (Figure 5c). It is also noticeable that in the same area where the sediments have undergone brittle faulting, contact metamorphic melting of the sediments mostly took place at dike/sediment contacts, whereas in the northern segment the anatexis of host rocks was more pervasive and is also found away from dike contacts. These observations, together with the prograde transformation of andalusite to sillimanite, suggest a significant increase in ambient temperatures from conditions where the deformation was brittle during the early nonmagmatic faulting stage to above 600 °C during the emplacement of the mafic dikes, contemporaneous with late stages of the stretching.

Three models can explain the temperature increase described above: (1) burial under the typical thickness of extrusive and intrusive volcanic rocks generally found at magma-rich rifted margins (SDR sequences of 3–7 km; Skogseid et al., 1992; Menzies et al., 2002), which, with a moderate geothermal gradient of 35 °C/km, would give a temperature increase of 105 to 245 °C; (2) related to volcanism at the margin, there is also an increased heat influx from the accumulation of lower crustal magma reservoirs and the introduction of dikes; and (3) condensation of geotherms during rift-related thinning of the continental crust. A combination of all or several of these factors is presumably the most likely scenario. Further studies to quantify the individual impact of these processes would be interesting, but are beyond the scope of this study.

The pressure data from the dike complex are intriguing, as some samples suggest relatively high pressure (i.e., 0.5 GPa for one Sarek sample), which indicates that the clinopyroxene crystals started crystallizing at greater depths than the others, possibly in a deeper magma reservoir. Crystallization in such a reservoir is likely also due to the evolved nature of the mafic dikes that have an average Mg# of 49.5 (see the supporting information) and thereby suggest that significant fractional crystallization of the mafic magma occurred prior to dike emplacement. Although such magma reservoirs have not been described from the Caledonides, they likely have a relatively small preservation potential during continental collision, due to their mafic composition and thereby dense nature. Furthermore, the distinctly older age of the granite than the dolerite at Corrovarre, and its implication of pervasive predike emplacement anatexis of the host sediments, suggests that an elevated geothermal gradient was established already before the main stage of mafic diking. Such excess heat at relatively shallow crustal levels is difficult to envisage without the effect of magmatism. The observations, radiometric ages, and *PT* analyses presented here may imply that magma was emplaced and stored within the lower crust prior to the main dike emplacement and thereby developed early in the rifting history. The existence of such early lower crustal magma reservoirs is also corroborated from modern examples of rifts and failed rifts, such as the main Ethiopia and Baikal rifts (Bastow et al., 2011; Nielsen & Thybo, 2009; Thybo et al., 2000).

6.2. Timing of Magmatism and Continental Breakup

In the North Atlantic Large Igneous Province (NALIP), continental breakup resulted in voluminous igneous activity generating both extrusives and intrusives into the sedimentary basin and underlying stretched continental crust. The magmatism was short lived and intense, with a peak lasting approximately 3 Myr (e.g., Menzies et al., 2002; Storey et al., 2007), consistent with other modern magma-rich rifted margins (Menzies et al., 2002).

By contrast, in the Scandinavian Caledonides, there is evidence for at least 20 Myr of rift-related magmatism preserved. The predominantly mafic magmatism, with its paucity of magmatic zircon and other datable minerals, and the variably strong Caledonian overprint complicate the documentation and precise dating of the evolution of the SDC. Ages of mafic magmatism obtained by CA-ID-TIMS generally fall within the time interval 608 to 596 Ma (Figure 2; Svenningsen, 2001; Baird et al., 2014; Kumpulainen et al., 2016),

suggesting that most of the SDC was emplaced during a short time period similar to the duration of the breakup of the NALIP. A younger SIMS age of 578 Ma has, however, also been found at Kebnekaise (Kirsch & Svenningsen, 2015).

The new zircon age for the crystallization of the Corrovarre dike swarm at 605.7 ± 1.8 Ma presented above (Figure 6) is similar to those in Kebnekaise and Sarek but older than the 570 and 560 Ma timing of the Seiland Igneous Complex (see Figure 2; Roberts et al., 2006, 2010) with which it was previously correlated (Zwaan & van Roermund, 1990). The new age for the Corrovarre dolerites as well as similarities in geochemistry (Roberts, 1990) documents that they are part of the SDC and can be correlated with the rest of the SDC in the southern segment. Tegner et al. (2019) have shown that, like the NALIP, the SDC was triggered by elevated upper mantle temperatures.

Opening of the Iapetus Ocean occurred in stages between about 620 and 550 Ma, beginning with rifting of rocks now found mainly in Caledonian nappes on Baltica and ending with breakup of southern Iapetus between Laurentia and Gondwana (Cawood et al., 2001). Rifting and opening of the portions of the Iapetus between Laurentia and Baltica is constrained by dating of mafic as well as felsic rift-related magmatic rocks in sedimentary basins and basement from both the Laurentian side (e.g., Dempster et al., 2002; Halliday et al., 1989; Kamo et al., 1989) and the Baltican side (Baird et al., 2014; Bingen et al., 1998; Kirsch & Svenningsen, 2015; Kumpulainen et al., 2016; Root & Corfu, 2012; Svenningsen, 2001; this study; Figure 11a). The oldest rift-related age on the Baltican side is that of the Egersund dikes, 616 ± 3 Ma (Bingen et al., 1998), whereas the youngest dikes at around 578 ± 9 Ma has been found in the Kebnekaise area (Kirsch & Svenningsen, 2015). However, many ages of both mafic and felsic magmatism fall between 608 and 596 Ma (Figure 11b), suggesting that although the magmatic record shows prolonged activity, the final breakup of Baltica and Laurentia was punctuated by a major dike emplacement event between 608 and 596 Ma.

6.3. Geodynamic Implication

The data presented above show that the intrusion of the 605.7 ± 1.8-Ma dolerites at Corrovarre was preceded by a widespread regional metamorphism coupled with a bedding-parallel stretching and anatexis of the host sediments (Figures 4a and 4b). Partial-melt migration and coalescence into granitoid veins, sills, and minor intrusive bodies occurred contemporaneously with the deformation (Lindahl et al., 2005; Zwaan & van Roermund, 1990; this study). The new granite age of 612.95 ± 0.93 Ma is similar to the age presented by Gee et al. (2016) of 610 ± 1 Ma from the Corrovarri granite but somewhat older than the 602 ± 5-Ma U-Pb zircon age presented by Corfu et al. (2007) for the nearby Rappesvarre granite. These ages coupled with field observations show that the host rock sediments were partially molten already prior to the main phase of dike emplacement (Figure 6d). In order to melt water-bearing sedimentary rocks at temperatures between 650 and 750 °C an elevated pressure is required (Figure 10). This agrees with the calculated crystallization pressure of 0.3 GPa presented here, and suggests that a high geotherm was established already prior to the emplacement of the SDC. Similar observations of S-type granites derived from water-present crustal anatexis have also been made in relatively shallow boreholes from the Vøring margin, offshore central Norway (Meyer et al., 2009), testifying to the high geothermal gradient at magma-rich rifted margins. Such partial melting has been proposed to constitute an important weakening process promoting continental breakup (Buiter & Torsvik, 2014). The new documentation presented here clearly shows that partial melting of host rocks prior to dike emplacement may have constituted the first step in a sequence of events with positive feedback leading to continental breakup.

From the data presented herein and elsewhere in the literature, we conclude that the structural and tectonothermal evolution of the Iapetus rifted margin in the Neoproterozoic can be summed up in four major events (see Figure 2 for timeline): (1) incipient stretching after approximately 850 Ma (Nystuen et al., 2008) and local magmatic activity (Paulsson & Andreasson, 2002; Walderhaug et al., 1999); (2) continuous or localized extension evolved through the Neoproterozoic with deposition of carbonates, sandstones, and eventually thick syn-rift clastic wedges (e.g., Kumpulainen & Nystuen, 1985; this period also included a few episodes of deposition of glaciogenic sediments); (3) as stretching continued, the crust thinned significantly and adiabatic melting of the upper mantle, associated with elevated lithosphere-asthenosphere temperatures, caused partial melting, LIP magmatism, and buildup of large mafic magma reservoirs at the base of the lithosphere (the stretching and the increased heat flux from incipient mafic intrusions in

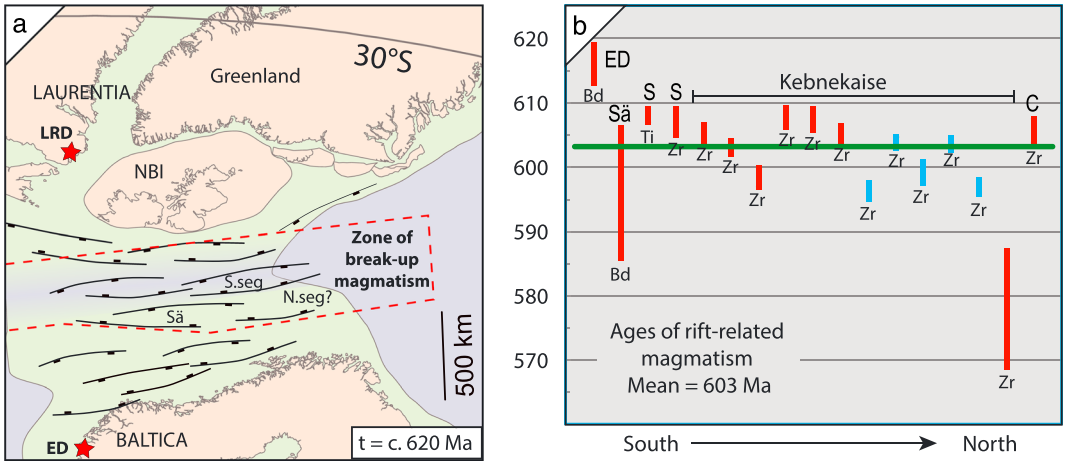

Figure 11. (a) Suggested paleogeographic reconstruction of Baltica and Laurentia at approximately 620 Ma, based on Tegner et al., 2019. Red stars show the locations of LRD and ED. (b) Overview of the age data from rift-related magmatism now preserved in the Scandinavian Caledonides. Ages of mafic dikes are colored red, whereas ages of granitoids are colored blue. ED = Egersund dikes; Sä = Särv; S = Sarek; S.seg = south segment; N.seg = northern segment; C = Corrovarre; Bd = Baddeleyite; Zr = Zircon; NBI = North British Isles.

the crust and the lower crustal reservoirs caused local pervasive melting of the host rock at approximately 610–612 Ma); (4) the plume-related Large Igneous Province (LIP) magmatism peaked at 608–596 Ma. This event produced large amounts of mafic dikes constituting ≥70–100% of the crustal volume. This event has been interpreted to represent the rift to drift transition and thus marks the opening of the Iapetus Ocean. This intense dike event and LIP magmatism probably also led to the rapid accumulation of thick (3–7 km) sequences of volcanics similar to present-day SDR, which presently are only sparsely preserved in the Scandinavian Caledonides.

7. Conclusions and Summary

It is demonstrated here that the mafic dikes at Corrovarre crystallized at 605.7 ± 1.8 Ma and thus have a similar crystallization age to the rest of the SDC further south. The SDC magmatism spans a relatively long period of time, but the peak mafic magmatism occurred between 608 and 596 Ma. This age span is interpreted to represent the opening of the Iapetus Ocean along the pre-Caledonian margin of Baltica.

Geothermobarometry from contact metamorphic host sediments (thermodynamic modeling and Ti-in-Bt) and the cross-cutting mafic dikes (jd-in-cpx-liq) suggests that the studied parts of the SDC were emplaced at 0.25 to 0.45 GPa and at temperatures of approximately 700 °C in the wall rocks, in areas where the dike density was most intense.

There was a significant increase in the geothermal gradient during the crustal extension from early, possibly coseismic brittle faulting during the nonmagmatic rifting stage to the thermal weakening and breakup triggered by the introduction of large volumes of plume generated mafic LIP magmas.

In the northern segment, crustal anatexis commenced already at 612–610 Ma, prior to dike emplacement. We interpret this temporal relation as being due to the formation of the pre-Caledonian LIP associated with the Central Iapetus Magmatic Province (Ernst & Bell, 2010). Accumulations of a lower crustal magma reservoir may have significantly heated parts of the extending crust.

Based on the new data presented and discussed here we suggest that the SDC represents the intermediate to lower levels of a distal magma-rich rifted margin invaded by LIP magmatism. More specifically, the dike swarms were probably feeding major volcanic systems, which are only locally preserved. The volcanic edifice was most likely a major component of the overburden. The abrupt increase in the geotherm and the prograde static metamorphic transformation (andalusite to sillimanite) of the initial contact metamorphic assemblages was associated with the LIP magmatism, which probably also was important for the lithospheric weakening that eventually resulted in continental breakup and seafloor spreading.

Acknowledgments

All the data that led to the conclusions of this article are presented in the figures, tables, and supporting information linked to the electronic version of this paper. This project was funded with the support from the Research Council of Norway through the Centre of Excellence funding scheme to CEED, project 223272 and the NFR-FRINAT project 25027 "Hyperextension in magma-poor and magma-rich domains along the pre-Caledonian passive margin of Baltica." This research was also funded by the Danish National Research Foundation Niels Bohr Professorship Grant 26-123/8 to C. T. We are indebted to Alex Zagorevski and David Chew for providing constructive reviews. The manuscript has improved significantly from their comments. Lars Augland is thanked for support in the TIMS lab; Sara Callegaro and David Neave are thanked for support with the *PT* estimates and Eric Tohver for support with SHRIMP analyses. National Park authorities in Norway and Sweden are acknowledged for the permissions to use helicopter to access remote areas in the parks.

References

Abdelmalak, M. M., Andersen, T. B., Planke, S., Faleide, J. I., Corfu, F., Tegner, C., et al. (2015). The ocean-continent transition in the mid-Norwegian margin: Insight from seismic data and an onshore Caledonian field analogue. *Geology*, *43*(11), 1011–1014. https://doi.org/10.1130/G37086.1

Abdelmalak, M. M., Faleide, J. I., Planke, S., Gernigon, L., Zastrozhnov, D., Shephard, G. E., & Myklebust, R. (2017). The T-reflection and the deep crustal structure of the Vøring margin, offshore mid-Norway. *Tectonics*, *36*, 2497–2523. https://doi.org/10.1002/2017TC004617

Andersen, T. B., Corfu, F., Labrousse, L., & Osmundsen, P.-T. (2012). Evidence for hyperextension along the pre-Caledonian margin of Baltica. *Journal of the Geological Society*, *169*(5), 601–612. https://doi.org/10.1144/0016-76492012-011

Andréasson, P.-G., Allen, A., Aurell, O., Boman, D., Ekestubbe, J., Goerke, U., et al. (2018). Seve terranes of the Kebnekaise Mts., Swedish Caledonides, and their amalgamation, accretion and affinity. *GFF*, *140*(3), 1–28.

Andréasson, P.-G., Svenningsen, O., Johansson, I., Solyom, Z., & Xiaodan, T. (1992). Mafic dyke swarms of the Baltica-Iapetus transition, Seve Nappe Complex of the Sarek Mts., Swedish Caledonides. *GFF*, *114*(1), 31–45.

Baird, G. B., Figg, S. A., & Chamberlain, K. R. (2014). Intrusive age and geochemistry of the Kebne Dyke complex in the Seve Nappe complex, Kebnekaise Massif, arctic Sweden Caledonides. *GFF*, *136*(4), 556–570. https://doi.org/10.1080/11035897.2014.924553

Bastow, I. D., & Keir, D. (2011). The protracted development of the continent-ocean transition in Afar. *Nature Geoscience*, *4*(4), 248–250. https://doi.org/10.1038/ngeo1095

Bastow, I. D., Keir, D., & Daly, E. (2011). The Ethiopia Afar Geoscientific Lithospheric Experiment (EAGLE): Probing the transition from continental rifting to incipient seafloor spreading. *Volcanism and evolution of the African lithosphere*, *478*, 1–26.

Bialas, R. W., Buck, W. R., & Qin, R. (2010). How much magma is required to rift a continent? *Earth and Planetary Science Letters*, *292*(1-2), 68–78. https://doi.org/10.1016/j.epsl.2010.01.021

Bingen, B., Demaiffe, D., & Breemen, O. V. (1998). The 616 Ma old Egersund basaltic dike swarm, SW Norway, and late Neoproterozoic opening of the Iapetus Ocean. *The Journal of Geology*, *106*(5), 565–574. https://doi.org/10.1086/516042

Brune, S. (2016). Rifts and rifted margins: A review of geodynamic processes and natural hazards. In *Plate Boundaries and Natural Hazards* (Chap. 2, Vol. 219, pp. 11–37). Hoboken, New Jersey: John Wiley. https://doi.org.10.1002/9781119054146.ch2

Buiter, S. J., & Torsvik, T. H. (2014). A review of Wilson Cycle plate margins: A role for mantle plumes in continental break-up along sutures? *Gondwana Research*, *26*(2), 627–653.

Cawood, P. A., McCausland, P. J., & Dunning, G. R. (2001). Opening Iapetus: Constraints from the Laurentian margin in Newfoundland. *Geological Society of America Bulletin*, *113*(4), 443–453. https://doi.org/10.1130/0016-7606(2001)113<0443:OICFTL>2.0.CO;2

Chew, D. M., & van Staal, C. R. (2014). The ocean-continent transition zones along the Appalachian–Caledonian margin of Laurentia: Examples of large-scale hyperextension during the opening of the Iapetus Ocean. *Geoscience Canada*, *41*(2), 165–185. https://doi.org/10.12789/geocanj.2014.41.040

Clemens, J. D., & Holness, M. B. (2000). Textural evolution and partial melting of arkose in a contact aureole: A case study and implications. *Visual Geosciences*, *5*(4), 1–14. https://doi.org/10.1007/s10069-000-0004-1

Clerc, C., Ringenbach, J.-C., Jolivet, L., & Ballard, J.-F. (2018). Rifted margins: Ductile deformation, boudinage, continentward-dipping normal faults and the role of the weak lower crust. *Gondwana Research*, *53*, 20–40. https://doi.org/10.1016/j.gr.2017.04.030

Corfu, F. (2004). U–Pb age, setting and tectonic significance of the anorthosite-mangerite-charnockite-granite suite, Lofoten-Vesterålen, Norway. *Journal of Petrology*, *45*(9), 1799–1819. https://doi.org/10.1093/petrology/egh034

Corfu, F., Gasser, D., & Chew, D. M. (2014). *New perspectives on the Caledonides of Scandinavia and related areas*. London: Geological Society of London. https://doi.org/10.1144/SP390.28

Corfu, F., Roberts, R. J., Torsvik, T., Ashwal, L. D., & Ramsay, D. M. (2007). Peri-Gondwanan elements in the Caledonian nappes of Finnmark, Northern Norway: Implications for the Paleogeographic framework of the Scandinavian Caledonides. *American Journal of Science*, *307*(2), 434–458. https://doi.org/10.2475/02.2007.05

Daniels, K. A., Bastow, I., Keir, D., Sparks, R., & Menand, T. (2014). Thermal models of dyke intrusion during development of continent-ocean transition. *Earth and Planetary Science Letters*, *385*, 145–153. https://doi.org/10.1016/j.epsl.2013.09.018

de Capitani, C., & Petrakakis, K. (2010). The computation of equilibrium assemblage diagrams with Theriak/Domino software. *American Mineralogist*, *95*(7), 1006–1016. https://doi.org/10.2138/am.2010.3354

Dempster, T., Rogers, G., Tanner, P., Bluck, B., Muir, R., Redwood, S., et al. (2002). Timing of deposition, orogenesis and glaciation within the Dalradian rocks of Scotland: Constraints from U-Pb zircon ages. *Journal of the Geological Society*, *159*(1), 83–94. https://doi.org/10.1144/0016-764901061

Direen, N. G., & Crawford, A. J. (2003). Fossil seaward-dipping reflector sequences preserved in southeastern Australia: A 600 Ma volcanic passive margin in eastern Gondwanaland. *Journal of the Geological Society*, *160*(6), 985–990. https://doi.org/10.1144/0016-764903-010

Eldholm, O. (1991). Magmatic tectonic evolution of a volcanic rifted margin. *Marine Geology*, *102*(1-4), 43–61. https://doi.org/10.1016/0025-3227(91)90005-O

Engel, A. J., & Engel, C. G. (1960). Progressive metamorphism and granitization of the major paragneiss, northwest Adirondack mountains, New York part II: Mineralogy. *Geological Society of America Bulletin*, *71*(1), 1–58. https://doi.org/10.1130/0016-7606(1960)71[1:PMAGOT]2.0.CO;2

Ernst, R. E., & Bell, K. (2010). Large igneous provinces (LIPs) and carbonatites. *Mineralogy and Petrology*, *98*(1-4), 55–76. https://doi.org/10.1007/s00710-009-0074-1

Faleide, J. I., Tsikalas, F., Breivik, A. J., Mjelde, R., Ritzmann, O., Engen, O., et al. (2008). Structure and evolution of the continental margin off Norway and the Barents Sea. *Episodes*, *31*(1), 82–91.

Gee, D. (1975). A tectonic model for the central part of the Scandinavian Caledonides. *American Journal of Science*, *275*, 468–515.

Gee, D. G., Andréasson, P.-G., Li, Y., & Krill, A. (2016). Baltoscandian margin, Sveconorwegian crust lost by subduction during Caledonian collisional orogeny. *GFF*, *139*(1), 1–16.

Geoffroy, L., Aubourg, C., Callot, J.-P., & Barrat, J.-A. (2007). Mechanisms of crustal growth in large igneous provinces: The North-Atlantic Province as a case study. *Geological Society of America Special Publication*, *430*, 747–774.

Gernigon, L., Ringenbach, J.-C., Planke, S., & Le Gall, B. (2004). Deep structures and breakup along volcanic rifted margins: Insights from integrated studies along the outer Vøring Basin (Norway). *Marine and Petroleum Geology*, *21*(3), 363–372. https://doi.org/10.1016/j.marpetgeo.2004.01.005

Gilotti, J. A., & Kumpulainen, R. (1986). Strain softening induced ductile flow in the Särv thrust sheet, Scandinavian Caledonides. *Journal of Structural Geology*, *8*(3-4), 441–455. https://doi.org/10.1016/0191-8141(86)90062-3

Hacker, B. R., Andersen, T. B., Johnston, S., Kylander-Clark, A. R., Peterman, E. M., Walsh, E. O., & Young, D. (2010). High-temperature deformation during continental-margin subduction & exhumation: The ultrahigh-pressure Western Gneiss Region of Norway. *Tectonophysics*, *480*(1-4), 149–171. https://doi.org/10.1016/j.tecto.2009.08.012

Halliday, A., Graham, C., Aftalion, M., & Dymoke, P. (1989). Short paper: The depositional age of the Dalradian Supergroup: U-Pb and Sm-Nd isotopic studies of the Tayvallich Volcanics, Scotland. *Journal of the Geological Society*, *146*(1), 3–6. https://doi.org/10.1144/gsjgs.146.1.0003

Henry, D. J., Guidotti, C. V., & Thomson, J. A. (2005). The Ti-saturation surface for low-to-medium pressure metapelitic biotites: Implications for geothermometry and Ti-substitution mechanisms. *American Mineralogist*, *90*(2-3), 316–328. https://doi.org/10.2138/am.2005.1498

Holbrook, W. S., Larsen, H., Korenaga, J., Dahl-Jensen, T., Reid, I. D., Kelemen, P., et al. (2001). Mantle thermal structure and active upwelling during continental breakup in the North Atlantic. *Earth and Planetary Science Letters*, *190*(3-4), 251–266. https://doi.org/10.1016/S0012-821X(01)00392-2

Hollocher, K., Robinson, P., Walsh, E., & Terry, M. P. (2007). The Neoproterozoic Ottfjället dike swarm of the middle allochthon, traced geochemically into the Scandian hinterland, Western Gneiss Region, Norway. *American Journal of Science*, *307*(6), 901–953. https://doi.org/10.2475/06.2007.02

Huang, W.-L., & Wyllie, P. (1981). Phase relationships of S-type granite with H_2O to 35 kbar: Muscovite granite from Harney Peak, South Dakota. *Journal of Geophysical Research*, *86*(B11), 10,515–10,529. https://doi.org/10.1029/JB086iB11p10515

Jakob, J., Alsaif, M., Corfu, F., & Andersen, T. B. (2017). Age and origin of thin discontinuous gneiss sheets in the distal domain of the magma-poor hyperextended pre-Caledonian margin of Baltica, southern Norway. *Journal of the Geological Society*, *174*(3), 557–571. https://doi.org/10.1144/jgs2016-049

Jakob, J., Andersen, T. B., & Kjøll, H. J. (2019). A review and reinterpretation of the architecture of the South and South-Central Scandinavian Caledonides—A magma-poor to magma-rich transition and the significance of the reactivation of rift inherited structures. *Earth-Science Reviews*, *192*, 513–528. https://doi.org/10.1016/j.earscirev.2019.01.004

Jamtveit, B., & Andersen, T. B. (1992). Morphological instabilities during rapid growth of metamorphic garnets. *Physics and Chemistry of Minerals*, *19*(3), 176–184.

Johannes, W. (1984). Beginning of melting in the granite system Qz-Or-Ab-An-H 2 O. *Contributions to Mineralogy and Petrology*, *86*(3), 264–273. https://doi.org/10.1007/BF00373672

Kamo, S. L., Gower, C. F., & Krogh, T. E. (1989). Birthdate for the Iapetus Ocean? A precise U-Pb zircon and baddeleyite age for the Long Range dikes, southeast Labrador. *Geology*, *17*(7), 602–605. https://doi.org/10.1130/0091-7613(1989)017<0602:BFTLOA>2.3.CO;2

Kelemen, P. B., & Holbrook, W. S. (1995). Origin of thick, high-velocity igneous crust along the US East Coast Margin. *Journal of Geophysical Research*, *100*(B6), 10,077–10,094. https://doi.org/10.1029/95JB00924

Kirsch, M., & Svenningsen, O. M. (2015). Root zone of a continental rift: The Neoproterozoic Kebnekaise Intrusive Complex, northern Swedish Caledonides. *GFF*, *138*(1), 31–53.

Kjøll, H. J., Galland, O., Labrousse, L., & Andersen, T. B. (2019). Emplacement mechanisms of a dyke swarm across the Brittle-Ductile transition and the geodynamic implications for magma-rich margins. *Earth and Planetary Science Letters*. https://doi.org/10.1016j.epsl.2009.04.16

Klausen, M. B., & Larsen, H. C. (2002). East Greenland coast-parallel dike swarm and its role in continental breakup. *Special paper-Geological Society of America*, *362*, 133–158.

Kullerud, K., Stephens, M., & Zachrisson, E. (1990). Pillow lavas as protoliths for eclogites: Evidence from a late Precambrian-Cambrian continental margin, Seve Nappes, Scandinavian Caledonides. *Contributions to Mineralogy and Petrology*, *105*(1), 1–10. https://doi.org/10.1007/BF00320962

Kumpulainen, R. (1980). Upper Proterozoic stratigraphy and depositional environments of the Tossåsfjället Group, Särv Nappe, southern Swedish Caledonides. *GFF*, *102*(4), 531–550.

Kumpulainen, R., & Nystuen, J. (1985). Late Proterozoic basin evolution and sedimentation in the westernmost part of Baltoscandia. *The Caledonide Orogen—Scandinavia and related areas*, *1*, 213–245.

Kumpulainen, R. A., Hamilton, M. A., Söderlund, U., and Nystuen, J. P., 2016, A new U-Pb baddeleyite age for the Ottfjället dolerite dyke swarm in the Scandinavian Caledonides—A minimum age for late Neoproterozoic glaciation in Baltica, Nordic Geologic Winter Meeting: Helsinki.

Lagabrielle, Y., Labaume, P., & de Saint Blanquat, M. (2010). Mantle exhumation, crustal denudation, and gravity tectonics during Cretaceous rifting in the Pyrenean realm (SW Europe): Insights from the geological setting of the lherzolite bodies. *Tectonics*, *29*, TC4012. https://doi.org/10.1029/2009TC002588

Lindahl, I., Stevens, B. P., & Zwaan, K. B. (2005). The geology of the Vaddas area, Troms: A key to our understanding of the Upper Allochthon in the Caledonides of northern Norway. *Norges Geologiske Undersøkelse*, *445*(5).

Majka, J., Be'eri-Shlevin, Y., Gee, D. G., Ladenberger, A., Claesson, S., Konecny, P., & Klonowska, I. (2012). Multiple monazite growth in the Åreskutan migmatite: Evidence for a polymetamorphic Late Ordovician to Late Silurian evolution in the Seve Nappe Complex of west-central Jamtland, Sweden. *Journal of Geosciences*, *57*(1), 3–23.

Manatschal, G. (2004). New models for evolution of magma-poor rifted margins based on a review of data and concepts from West Iberia and the Alps. *International Journal of Earth Sciences*, *93*(3), 432–466.

Manatschal, G., & Müntener, O. (2009). A type sequence across an ancient magma-poor ocean–continent transition: The example of the western Alpine Tethys ophiolites. *Tectonophysics*, *473*(1-2), 4–19. https://doi.org/10.1016/j.tecto.2008.07.021

Menzies, M. A., Klemperer, S. L., Ebinger, C. J., & Baker, J. (2002). Characteristics of volcanic rifted margins. In M. A. Menzies, S. L. Klemperer, C. J. Ebinger, & J. Baker (Eds.), *Volcanic Rifted Margins* (Vol. 362, pp. 119–132). Boulder, CO: Geological Society of America.

Meyer, R., Hertogen, J., Pedersen, R. B., Viereck-Götte, L., & Abratis, M. (2009). Interaction of mantle derived melts with crust during the emplacement of the Vøring Plateau, NE Atlantic. *Marine Geology*, *261*(1-4), 3–16. https://doi.org/10.1016/j.margeo.2009.02.007

Mohn, G., Manatschal, G., Beltrando, M., & Haupert, I. (2014). The role of rift-inherited hyper-extension in Alpine-type orogens. *Terra Nova*, *26*(5), 347–353. https://doi.org/10.1111/ter.12104

Neave, D. A., & Putirka, K. D. (2017). A new clinopyroxene-liquid barometer, and implications for magma storage pressures under Icelandic rift zones. *American Mineralogist*, *102*(4), 777–794. https://doi.org/10.2138/am-2017-5968

Nielsen, C., & Thybo, H. (2009). Lower crustal intrusions beneath the southern Baikal Rift Zone: Evidence from full-waveform modelling of wide-angle seismic data. *Tectonophysics*, *470*(3-4), 298–318. https://doi.org/10.1016/j.tecto.2009.01.023

Nystuen, J. P., Andresen, A., Kumpulainen, R. A., & Siedlecka, A. (2008). Neoproterozoic basin evolution in Fennoscandia, East Greenland and Svalbard. *Episodes*, *31*(1), 35–43.
Paulsson, O., & Andreasson, P.-G. (2002). Attempted break-up of Rodinia at 850 Ma: Geochronological evidence from the Seve-Kalak Superterrane, Scandinavian Caledonides. *Journal of the Geological Society*, *159*(6), 751–761. https://doi.org/10.1144/0016-764901-156
Planke, S., Symonds, P. A., Alvestad, E., & Skogseid, J. (2000). Seismic volcanostratigraphy of large-volume basaltic extrusive complexes on rifted margins. *Journal of Geophysical Research*, *105*(B8), 19,335–19,351. https://doi.org/10.1029/1999JB900005
Putirka, K. D. (2008). Thermometers and barometers for volcanic systems. *Reviews in Mineralogy and Geochemistry*, *69*(1), 61–120. https://doi.org/10.2138/rmg.2008.69.3
Roberts, D. (1990). Geochemistry of mafic dykes in the Corrovarre nappe, Troms, North Norway. *Norges geologiske undersøkelse Bulletin*, *419*, 45–54.
Roberts, R., Corfu, F., Torsvik, T., Ashwal, L., & Ramsay, D. (2006). Short-lived mafic magmatism at 560–570 Ma in the northern Norwegian Caledonides: U-Pb zircon ages from the Seiland Igneous Province. *Geological Magazine*, *143*(6), 887–903. https://doi.org/10.1017/S0016756806002512
Roberts, R. J., Corfu, F., Torsvik, T., Hetherington, C. J., & Ashwal, L. D. (2010). Age of alkaline rocks in the Seiland Igneous Province, Northern Norway. *Journal of the Geological Society*, *167*(1), 71–81. https://doi.org/10.1144/0016-76492009-014
Root, D., & Corfu, F. (2012). U–Pb geochronology of two discrete Ordovician high-pressure metamorphic events in the Seve Nappe Complex, Scandinavian Caledonides. *Contributions to Mineralogy and Petrology*, *163*(5), 769–788. https://doi.org/10.1007/s00410-011-0698-0
Skogseid, J., Pedersen, T., Eldholm, O., & Larsen, B. T. (1992). Tectonism and magmatism during NE Atlantic continental break-up: The Vøring Margin. *Geological Society, London, Special Publications*, *68*(1), 305–320. https://doi.org/10.1144/GSL.SP.1992.068.01.19
Smith, D. C. (1984). Coesite in clinopyroxene in the Caledonides and its implications for geodynamics. *Nature*, *310*(5979), 641–644. https://doi.org/10.1038/310641a0
Stab, M., Bellahsen, N., Pik, R., Quidelleur, X., Ayalew, D., & Leroy, S. (2016). Modes of rifting in magma-rich settings: Tectono-magmatic evolution of Central Afar. *Tectonics*, *35*, 2–38. https://doi.org/10.1002/2015TC003893
Stølen, L. K. (1994). The rift-related mafic dyke complex of the Rohkunborri Nappe, Indre Troms, northern Norwegian Caledonides. *Norsk Geologisk Tidsskrift*, *74*, 35–47.
Storey, M., Duncan, R. A., & Tegner, C. (2007). Timing and duration of volcanism in the North Atlantic Igneous Province: Implications for geodynamics and links to the Iceland hotspot. *Chemical Geology*, *241*(3-4), 264–281. https://doi.org/10.1016/j.chemgeo.2007.01.016
Svenningsen, O. M. (1994a). The Baltica–Iapetus passive margin dyke complex in the Sarektjåkkå Nappe, northern Swedish Caledonides. *Geological Journal*, *29*(4), 323–354.
Svenningsen, O. M. (1994b). Tectonic significance of the meta-evaporitic magnesite and scapolite deposits in the Seve Nappes, Sarek Mts., Swedish Caledonides. *Tectonophysics*, *231*(1-3), 33–44. https://doi.org/10.1016/0040-1951(94)90119-8
Svenningsen, O. M. (2001). Onset of seafloor spreading in the Iapetus Ocean at 608 Ma: precise age of the Sarek Dyke Swarm, northern Swedish Caledonides. *Precambrian Research*, *110*(1-4), 241–254. https://doi.org/10.1016/S0301-9268(01)00189-9
Tegner, C., Andersen, T. B., Kjøll, H. J., Brown, E. L., Hagen-Peter, G., Corfu, F., et al. (2019). A mantle Plume origin for the Scandinavian Dyke Complex: A "piercing point" for the 615 Ma plate reconstruction of Baltica? *Geochemistry, Geophysics, Geosystems*, *20*(2), 1075–1094. https://doi.org/10.1029/2018GC007941
Theissen-Krah, S., Zastrozhnov, D., Abdelmalak, M., Schmid, D., Faleide, J., & Gernigon, L. (2017). Tectonic evolution and extension at the Møre margin-offshore mid-Norway. *Tectonophysics*, *721*, 227–238. https://doi.org/10.1016/j.tecto.2017.09.009
Thybo, H., Maguire, P., Birt, C., & Perchuć, E. (2000). Seismic reflectivity and magmatic underplating beneath the Kenya Rift. *Geophysical Research Letters*, *27*(17), 2745–2748. https://doi.org/10.1029/1999GL011294
van Wijk, J., Koning, D., Axen, G., Coblentz, D., Gragg, E., & Sion, B. (2018). Tectonic subsidence, geoid analysis, and the Miocene-Pliocene unconformity in the Rio Grande rift, southwestern United States: Implications for mantle upwelling as a driving force for rift opening. *Geosphere*, *14*(2), 684–709. https://doi.org/10.1130/GES01522.1
Walderhaug, H. J., Torsvik, T. H., Eide, E. A., Sundvoll, B., & Bingen, B. (1999). Geochronology and palaeomagnetism of the Hunnedalen dykes, SW Norway: Implications for the Sveconorwegian apparent polar wander loop. *Earth and Planetary Science Letters*, *169*(1-2), 71–83. https://doi.org/10.1016/S0012-821X(99)00066-7
Weinberg, R. F., & Regenauer-Lieb, K. (2010). Ductile fractures and magma migration from source. *Geology*, *38*(4), 363–366. https://doi.org/10.1130/G30482.1
White, L. T., & Ireland, T. R. (2012). High-uranium matrix effect in zircon and its implications for SHRIMP U–Pb age determinations. *Chemical Geology*, *306*, 78–91.
White, R., Smith, L., Roberts, A., Christie, P., Kusznir, N., Roberts, A., et al. (2008). Lower-crustal intrusion on the North Atlantic continental margin. *Nature*, *452*(7186), 460–464. https://doi.org/10.1038/nature06687
White, R. S., Spence, G. D., Fowler, S. R., McKenzie, D. P., Westbrook, G. K., & Bowen, A. N. (1987). Magmatism at rifted continental margins. *Nature*, *330*(6147), 439–444. https://doi.org/10.1038/330439a0
Whitney, D. L., & Evans, B. W. (2010). Abbreviations for names of rock-forming minerals. *American Mineralogist*, *95*(1), 185–187. https://doi.org/10.2138/am.2010.3371
Zastrozhnov, D., Gernigon, L., Gogin, I., Abdelmalak, M., Planke, S., Faleide, J., et al. (2018). Cretaceous-Paleocene evolution and crustal structure of the northern Vøring margin (offshore mid-Norway): Results from Integrated Geological and Geophysical Study. *Tectonics*, *37*, 497–528. https://doi.org/10.1002/2017TC004655
Zwaan, B. K., & van Roermund, H. L. (1990). A rift-related mafic dyke swarm in the Corrovarre Nappe of the Caledonian Middle Allochthon, Troms, North Norway, and its tectonometamorphic evolution. *Norges geologiske undersøkelse Bulletin*, *419*, 25–44.